Recurrent urinary tract infection and estrogen shape the taxonomic ecology and functional potential of the postmenopausal urobiome

Michael L. Neugent[1], Ashwani Kumar[2], Neha V. Hulyalkar[1], Kevin C. Lutz[3], Vivian H. Nguyen[1], Jorge L. Fuentes[4], Cong Zhang[3], Amber Nguyen[1], Belle M. Sharon[1], Amy Kuprasertkul[4], Amanda P. Arute[1], Tahmineh Ebrahimzadeh[1], Nitya Natesan[1], Qiwei Li[3], Chao Xing[2,5,6], Vladimir Shulaev[7,8], Philippe E. Zimmern[4], Kelli L. Palmer[1], Nicole J. De Nisco[1,4#]

[1]Department of Biological Sciences, The University of Texas at Dallas, Richardson, TX
[2]Eugene McDermott Center for Human Growth and Development, The University of Texas Southwestern Medical Center, Dallas, TX
[3]Department of Mathematical Sciences, The University of Texas at Dallas, Richardson, TX
[4]Department of Urology, The University of Texas Southwestern Medical Center, Dallas, TX
[5]Department of Bioinformatics, The University of Texas Southwestern Medical Center, Dallas, TX
[6]Department of Population and Data Sciences, The University of Texas Southwestern Medical Center, Dallas, TX
[7]Department of Biological Sciences, The University of North Texas, Denton, TX
[8]Advanced Environmental Research Institute, The University of North Texas, Denton, TX

[#]Please address correspondence to Nicole De Nisco, nicole.denisco@utdallas.edu

Keywords: urobiome, metagenomics, estrogen, urinary tract infection

Running Title: Estrogen and rUTI history shape the urobiome of postmenopausal women

Abstract

Community-acquired urinary tract infection (UTI) is among the most common bacterial infections observed in humans. Postmenopausal women are a rapidly growing and underserved demographic group who are severely affected by recurrent UTI (rUTI) with a >50% recurrence rate. In this population, rUTI can persist for years, reducing quality of life and imposing a significant healthcare burden. rUTI is most often treated by antibiotics, but development of antibiotic resistance and allergy limit therapeutic options. The female urinary microbiome (urobiome) has been identified as a key component of the urogenital environment. However, compositional and functional changes in the urobiome underlying rUTI susceptibility in postmenopausal women are not well understood. Here, we used a controlled, cross-sectional cohort of postmenopausal women, to interrogate changes in urobiome structure and function linked to rUTI susceptibility by whole genome metagenomic sequencing (WGMS), advanced urine culture, estrogen metabolite profiling, and antibiotic sensitivity testing. Overall, we detected 276 bacterial, archaeal, and fungal species representing 106 genera. We find a putative commensal population consisting of species known to protect against bacterial vaginosis, such as *Lactobacillus crispatus*, within the urobiome of postmenopausal women who do not experience UTI. Integration of clinical metadata detected an almost exclusive enrichment of lactobacilli, including *L. crispatus* and *L. vaginalis,* in women taking estrogen hormone therapy (EHT). Integrating quantitative metabolite profiling of urinary estrogens with WGMS, we observed robust correlations between urobiome taxa, such as *Bifidobacterium breve* and *L. crispatus*, and urinary estrogen conjugate concentrations in women with no history of UTI that were absent in women with rUTI history. We further used functional metagenomic profiling and patient-derived isolate phenotyping to identify microbial metabolic pathways, antimicrobial resistance genes (ARGs), and clinically relevant antimicrobial resistance phenotypes enriched between disease-states. Our data indicate that distinct urobiome metabolic and ARG signatures are associated with current rUTI status and history. Importantly, we observed that rUTI history leaves an imprint of enriched ARGs even in women not currently experiencing UTI. Taken together, our data suggests that rUTI history and estrogen strongly shape the functional and taxonomic composition of the urobiome in postmenopausal women.

Introduction

Urinary tract infection (UTI) is among the most common adult bacterial infections and imparts a particularly significant medical burden on women, with more than 50% of women suffering UTI in their lifetime (Gaitonde et al., 2019; Jhang and Kuo, 2017). Historically, UTI has largely been underprioritized in medical research due to low mortality rates and the effectiveness of available

antibiotics. However, UTI is a disease of disproportionate burden as age is one of the strongest associated risk factors for UTI and the development of recurrent UTI (rUTI) (Flores-Mireles et al., 2015). Indeed, approximately 50% of UTIs in postmenopausal (PM) women develop into rUTI, which is clinically defined as ≥3 symptomatic UTIs in 12 months (Gaitonde et al., 2019; Malik et al., 2018b). rUTI can last for years, dramatically decreasing quality of life and, if treatment is unsuccessful, can develop into life-threatening urosepsis. Current therapeutic strategies rely on the use of antibiotics to achieve urinary tract sterility (Flores-Mireles et al., 2015; Malik et al., 2018a; Neugent et al., 2020). However, increasing rates of antibiotic refractory rUTI make this strategy unsustainable and ultimately ineffective (Malik et al., 2018a). Alternate therapeutic strategies are therefore needed to increase quality of life and reduce adverse outcomes for women with rUTI.

A promising source of therapeutic strategies for rUTI lies in modulating or restoring the urinary microbiome, termed here the “urobiome” (Stamm and Norrby, 2001; Wolfe and Brubaker, 2019). Decades of medical dogma have largely assumed sterility of urine and the urinary tract; however, a large body of work has robustly established the existence of a human urobiome (Brubaker and Wolfe, 2017; Hilt et al., 2014; Lewis et al., 2013; Price et al., 2019; Siddiqui et al., 2011; Wolfe et al., 2012). Initial taxonomic analyses have associated urobiome compositional dysbiosis with urinary incontinence, overactive bladder, and bladder cancer (Bucevic Popovic et al., 2018; Karstens et al., 2016; Pearce et al., 2014). Still, fundamental knowledge of urobiome composition and function in PM women, especially in the context of rUTI susceptibility, is lacking. Studies surveying the microbial ecologies of the urobiome associated with UTI have almost exclusively focused on premenopausal women or cohorts of mixed age (Barraud et al., 2019; Brubaker and Wolfe, 2017; Hilt et al., 2014; Neugent et al., 2020; Price et al., 2019; Siddiqui et al., 2011; Wolfe et al., 2012). As a result, the relationship between the urobiome and rUTI susceptibility is poorly understood in PM women. A 2021 report showed that premenopausal and PM women displayed different core urinary microbiota at the genus level, providing strong rationale to characterize the PM urobiome in urogenital disease (Ammitzboll et al., 2021).

The female urobiome is reported to be interconnected with the vaginal microbiome (Thomas-White et al., 2018). For example, D(-)Lactate-producing lactobacilli, known to protect the vagina from colonization by bacterial and fungal pathogens, have been consistently observed in the female urobiome in multiple independent studies (Edwards et al., 2019; Pearce et al., 2014). These observations beg the question of whether these known protective vaginal species serve a similar role in the urobiome. A 2011 clinical trial found a moderate reduction of rUTI incidence among women receiving an intravaginal *L. crispatus* probiotic (Stapleton et al., 2011). While this

study was performed in premenopausal women and has yet to be confirmed in a larger clinical study, it does suggest that lactobacilli may support urinary tract health.

To date, no whole genome metagenomic sequencing (WGMS) datasets have been generated to profile the urobiome of PM women. Given the genomic diversity observed within and among taxonomic clades, metagenomic information beyond 16S rRNA sequence enrichment is needed to assess the functional potential of microbial communities (Quince et al., 2017). Whole-metagenome analysis of the urobiome is required to identify the genes and metabolic pathways associated with urinary tract health. Here, we present a WGMS survey of the urobiome of a strictly curated, cross-sectional cohort of PM women separated into three groups defined by rUTI history and current UTI status. Taxonomic biomarker analysis detected a microbial signature that suggests an imprint of past UTI remains in the urobiome. We also observed a striking association between the use of estrogen hormone therapy (EHT) and the presence of vaginal lactobacilli in the urobiome. Further, we observed strong *Lactobacillus* enrichment among women using oral and patch EHT, but not women using vaginal EHT. These findings mirror the detected concentrations of excreted urinary estrogen metabolites in women using EHT, which we found positively correlated with abundances of potentially protective urinary taxa in women with no UTI history. Finally, we found that the resistome of the urinary microbiota is dramatically altered in women with rUTI history even in the absence of active infection. Taken together, these results suggest that both urobiome taxonomy and functional potential are shaped by rUTI history and EHT in PM women.

Results

Cohort curation, metagenomic DNA preparation, and whole genome metagenomic dataset generation

rUTI often follows a cyclic pattern of infection (relapse) interrupted by periods of remission (Figure 1A). To model this pattern of relapse and remission, PM women were striated into three groups based on rUTI history. Group 1 served as a healthy comparator and consisted of PM women with no lifetime history of symptomatic UTI (No UTI History), group 2 consisted of PM women with a recent history of rUTI but no active UTI at the time of urine donation (rUTI Remission), and group 3 consisted of PM women with a history of rUTI and an active, symptomatic UTI at the time of urine donation (rUTI Relapse) (Figure 1B). All recruited women passed strict inclusion criteria for uncomplicated rUTI. We determined that 25 women per group were sufficient to balance *a-priori* sample size estimation (Figure S 1A, B) with clinical feasibility and enrollment rates. The final cohort was balanced for sample size, Race, BMI, smoking history, EHT use, urine

137 pH, and urinary creatinine concentration. It should be noted the women in the rUTI Relapse group
138 tended to be older with a median age of 76 compared to 67 in the No UTI History and 68 in the
139 rUTI Remission groups (Table S1).
140 Urine was collected via the clean-catch midstream method and is therefore representative of
141 the urogenital microbiome (Karstens et al., 2018), which is includes the bladder, urethral, and, in
142 some cases, vaginal microbiomes. Metagenomic DNA yields reflected the anticipated biomass of
143 the urobiome in each group with the highest DNA yields observed in the rUTI Relapse group
144 (Figure S 1C). We observed an average of 67.6% host contamination within the WGMS data
145 (Figure S 1D). Previous reports of human contamination in WGMS sequencing of the urobiome
146 range from 1-99% of obtained reads (Moustafa et al., 2018; Quince et al., 2017). To measure
147 potential background and environmental taxonomic signals, a pure water sample was randomly
148 inserted into the metagenomic DNA isolation and sequencing workflow (Segata et al., 2012). Most
149 microbial reads observed in the water control mapped to common nucleic acid purification kit and
150 environmental contaminants (Figure S 2A) (Salter et al., 2014). Except for known members of the
151 human microbiome, these background taxa were censored from the data.
152
153 **Validation of viable urobiome species through advanced urine culture and WGMS hybrid**
154 **taxonomic profiling.**
155 To validate the presence of living microbiota within the urobiomes sampled, we coupled WGMS
156 with advanced urine culture, a modification of the previously reported enhanced quantitative urine
157 culture protocol (Price et al., 2016). Taxonomic profiling by WGMS detected 276 bacterial,
158 archaeal, and fungal species across 106 genera within the aggregate urobiome of all three
159 groups. The sampled urobiomes were dominated by the kingdom, Bacteria, which represented
160 99.4% of the detected non-viral, microbial taxa (Figure 1C). Consistent with the observed
161 taxonomic composition of urobiomes studied to date (Brubaker and Wolfe, 2017; Siddiqui et al.,
162 2011), the detected bacterial taxa across the cohort belonged to four major phyla: Firmicutes
163 (44.7%), Actinobacteria (22.3%), Proteobacteria (20.6%), and Bacteroidetes (12%) (Figure 1C).
164 Advanced urine culture captured 93.9% of bacterial genera detected in WGMS with observed
165 aggregate relative abundance ≥5% in any sample (Figure 1D). Patient-level culture coverage is
166 reported in Figure S 2A. The most frequent cultivable genera across all samples were
167 *Lactobacillus*, *Escherichia*, *Streptococcus*, *Bifidobacterium*, *Gardnerella*, *Klebsiella*,
168 *Staphylococcus*, *Finegoldia*, *Enterococcus*, and *Facklamia*. Pure isolates from every cultivable
169 species were assembled into a biobank of 896 bacterial and fungal isolates.
170

171 **rUTI History is not associated with large-scale alterations of urobiome ecological structure**
172 **in the absence of active infection.**
173 We next analyzed the genus and species-level taxonomic profiles within the No UTI History,
174 rUTI Remission and rUTI Relapse groups (Figure 2A, B, Figure S 3A). rUTI Relapse group
175 urobiomes were mainly dominated by single bacterial uropathogens with little detected
176 abundance of Fungi and *Archaea* (Figure 2B, Figure S 3A). The most prevalent bacterium was
177 *Escherichia coli* (15/25, 60%), the major uropathogen among most types of UTI (Flores-Mireles
178 et al., 2015). Along with *E. coli*, we detected known uropathogens, *Klebsiella pneumoniae* (2/25,
179 8%), *Enterococcus faecalis* (1/25, 4%), and *Streptococcus agalactiae* (1/25, 4%). We observed a
180 low relative abundance of fungal species within the rUTI Relapse urobiomes including *Candida*
181 *glabrata* and *Malassenzia globosa*. Similarly low relative abundances of archaeal taxa were
182 detected, such as, *Methanobrevibacter spp.* (Figure S 3A). The most observed viral taxa were JC
183 polyomavirus (4/25 16%) but Human herpes virus 4 (1/25 4%) and Enterobacteria phage lke (1/25
184 4%) were also detected (Figure S 3B).
185 The most frequently observed bacterial species in urobiomes of women without active UTI (No
186 UTI History and rUTI Remission) belonged to the genera *Lactobacillus*, *Bifidobacterium*,
187 *Gardnerella*, *Streptococcus*, *Staphylococcus*, and *Actinobaculum* (Figure 2 A, B). A subset of
188 these samples (54%) was dominated by one taxon while others were diverse and exhibited no
189 single dominant taxon. We observed 13 patients (24%) in the No UTI History and rUTI Remission
190 groups with a >50% relative abundance of various *Lactobacillus spp*., including *L. crispatus, L.*
191 *iners*, and *L. gasseri* (Figure 2B). Interestingly, we also observed a subset of urobiomes in the No
192 UTI History and rUTI Remission groups dominated by *Bifidobacterium spp.*, such as *B. breve, B.*
193 *dentium*, and *B. longum*, as well as by *Gardnerella vaginalis* (Figure 2B). Fungal and archaeal
194 species were observed in low abundance (0-8.8% relative abundance) in the No UTI History and
195 rUTI Remission urobiomes and included *Candida albicans*, *C. glabrata*, and *Candida dubliniensis,*
196 as well as *M. globosa*, *Naumovozyma spp.*, and *Eremothecium spp* (Figure S 3A). Observed
197 archaeal species within the No UTI History and rUTI Remission urobiomes included
198 *Methanosphaera stadtmanae* and *Methanobrevibacter spp.* Viral taxa were more frequently
199 observed in the No UTI history and rUTI Remission groups than in the rUTI Relapse group and
200 included JC, BK, and Merkel cell polyomaviruses (Figure S 3B).
201 To model the urobiome ecological structure within the three groups, we calculated alpha-
202 diversity indices including the observed taxa count, Shannon, Simpson, Chao 1, and ACE indices.
203 Women in the No UTI History and rUTI Remission groups had similarly diverse urobiomes across
204 different indices (Figure 2C, D, Figure S 4 A, B, C). These data suggest that if there are differences

205 in the urobiomes of PM women who are susceptible to rUTI (rUTI Remission) versus those who
206 are not (No UTI History), they are not reflected in alpha-diversity metrics. The rUTI Relapse group
207 exhibited significantly lower alpha-diversity as compared to the rUTI Remission cohort (Figure 2C,
208 D, Figure S 4 A, B, C).
209 To assess large-scale taxonomic signatures associated with rUTI, we used double principal
210 coordinate analysis (DPCoA) (Pavoine et al., 2004). Visualization of the first two PCoAs revealed
211 that the urobiomes of the rUTI Relapse group clustered along a vector defined by *E. coli* and were
212 ecologically distinct from the urobiomes of the No UTI History and rUTI Remission groups. The
213 No UTI History and rUTI Remission groups exhibited relatively similar clustering patterns in the
214 first two PCoAs (Figure 2E), and clustered along opposing vectors defined by the enrichment of
215 either *L. crispatus* or *G. vaginalis*, which are associated with a healthy vaginal microbiome or
216 bacterial vaginosis, respectively (Ravel and Brotman, 2016; Ravel et al., 2011). This similar
217 clustering of the No UTI history and rUTI Remission cohorts suggests that a history of rUTI does
218 not significantly alter the large-scale taxonomic structure of the urobiome in PM women.
219
220 **Taxonomic profile of the PM urobiome displays co-occurrence structure.**
221 Microbial communities can harbor intricate interactions between member taxa (Alteri et al.,
222 2015; Keogh et al., 2016). Exceedingly little is known about interactions and co-occurrence of
223 bacterial species within the urobiome. We performed taxonomic association analysis to determine
224 the co-occurrence structure of the PM urobiome and identified 87 statistically significant genus-
225 level associations ($P<0.05$) (Figure 2F). After multiple hypothesis testing correction, a total of 17
226 unique associations exhibited robust statistical significance ($Q<0.05$) (Figure 2F). Network
227 visualization of significant positive associations ($P<0.05$) revealed 3 non-interacting microbial
228 clusters (Figure 2G). Cluster 1 member taxa included genera previously associated with vaginal
229 infections, such as *Bacteroides* and *Blautia* (Ceccarani et al., 2019). Cluster 2 exhibited the
230 largest member set and diversity, and captured associations between genera known to inhabit
231 the urobiome (i.e. *Peptoniphilus* and *Finegoldia*) but whose association has not yet been reported
232 (Anglim et al., 2021; Thomas-White et al., 2017). Cluster 2 grouped strongly around the genus
233 *Peptoniphilus.* Cluster 3 was identified as a pairwise interaction between the genera *Gardnerella*
234 and *Atopobium*, two taxa that are associated in vaginal dysbiosis and bacterial vaginosis
235 (Bradshaw et al., 2006; Hardy et al., 2016; Hardy et al., 2015). We also observed anticorrelated
236 taxa (Figure 2 F, Figure S 4 D). The two main hubs of the negative correlation network were the
237 genera *Lactobacillus* and *Escherichia*. Of note, the most significant negative association was
238 observed between the *Lactobacillus* and *Peptoniphilus* (Figure 2 F, Figure S 4 D). Taken together,

239 these data define patterns of co-occurrence within the urobiome and suggest candidate taxa, (i.e.
240 *Lactobacillus*, *Peptoniphilus*, and *Escherichia)* that may act as hubs of community structure.
241

242 **Taxonomic biomarker analysis reveals that rUTI history alters the species-level taxonomic**
243 **signature of the urobiome.**

244 Although we did not detect large scale taxonomic differences between the rUTI Remission and
245 No UTI History groups, we hypothesized that small scale differences (e.g. enrichment of a single
246 genus or species) may contribute to differential rUTI susceptibility between groups. We therefore
247 performed genus and species-level differential taxonomic enrichment analysis between the No
248 UTI History and rUTI Remission urobiomes using both linear discriminant analysis of effect size
249 (LEfSe) and a Bayesian microbial differential abundance (BMDA) model (Li et al., 2019; Segata
250 et al., 2011). While LEfSe performs a non-parametric assessment of differential abundance,
251 BMDA can account for sparsity, over-dispersion, and uneven sampling depth. Though LEfSe
252 detected no differentially abundant taxa between the No UTI History and rUTI Remission groups,
253 BMDA detected multiple differentially abundant taxa. BMDA detected two genera, *Aerococcus*
254 and *Lactobacillus*, as well as two species of lactobacilli, *L. vaginalis* and *L. crispatus*, as enriched
255 in the No UTI History group (Figure 3A, B). At the genus-level, *Klebsiella*, *Gemella*, *Bacteroides*,
256 *Clostridiales Family XIII Incertae Sedis unclassified*, *Eggerthella*, and *Escherichia* were among
257 the most significantly enriched in the rUTI Remission group. Fifteen species were identified as
258 significantly enriched in the rUTI Remission group, including *Ureaplasma parvum*, *Bacteroides*
259 *uniformis*, *Brevibacterium massiliense*, *Anaerococcus hydrogenalis*, *Actinomyces turicensis*,
260 *Prevotella timonensis*, *E. faecalis*, *Staphylococcus hominis*, *Peptoniphilus lacrimalis*,
261 *Corynebacterium pseudogenitalium*, *Actinomyces europeaus*, *Facklamia hominis*, *Finegoldia*
262 *magna*, *Anaerococcus prevotii*, and *Staphylococcus epidermidis* (Figure 3B). Many of these taxa,
263 such as the genera *Bacteroides*, *Streptococcus*, *Escherichia*, *Ureaplasma*, *Finegoldia*, and
264 *Gemella*, have been found in the vaginal microbiome during infection (Ceccarani et al., 2019;
265 Shipitsyna et al., 2013) . Furthermore, *A. turicensis* and *A. europaeus* are known to be associated
266 with UTI (Kononen and Wade, 2015). Taken together, these results suggest that rUTI history may
267 leave an imprint on urobiome composition that may be missed by common ecological indices
268 (alpha or beta diversity) and differential abundance pipelines that do not consider the sparsity,
269 over-dispersion and uneven sampling that is common in low biomass microbiomes like the
270 urobiome (Karstens et al., 2018).
271

272 **Urobiome taxonomic structure differs in women using estrogen hormone therapy**

273 Given that many of the urobiomes of women without active rUTI were dominated by species of
274 lactobacilli (26%, 13/50) (Figure 2 A, B), we sought to further characterize this taxonomic
275 enrichment in the No UTI History and rUTI Remission groups. We screened the cohort-associated
276 clinical metadata for variables associated with *Lactobacillus* abundance. Interestingly, we found
277 that estrogen hormone therapy (EHT) was strongly associated with the presence of *Lactobacillus*
278 in the urobiome (Figure 4 A, B, C). Ecological modeling revealed that the urobiomes of EHT(+)
279 women were significantly less diverse than those of EHT(-) women and tended to be dominated
280 by a single species of lactobacilli (Figure 4 D, E, F). To identify taxa associated with EHT use, we
281 performed differential taxonomic enrichment analysis using LEfSe and BMDA. Notably, LEfSe
282 found an enrichment of the genus *Lactobacillus* in EHT(+) women and the genus *Streptococcus*,
283 and EHT(-) women (Figure 4 G). BMDA captured a similar result but further resolved species-
284 level differential enrichment (Figure 4 H). *L. crispatus* and *L. vaginalis*, were significantly enriched
285 in the urobiomes of EHT(+) women and *Streptococcus mitis/oralis/pneumoniae* (*S. m/o/p*) group,
286 *Streptococcus infantis*, and *Atopobium vaginae* were enriched in the EHT(-) group (Figure 4H).
287

288 **Urinary estrogen concentration is positively correlated with urobiome *Lactobacillus***
289 **abundance in PM women with No UTI history**

290 EHT can be administered via multiple modalities including oral supplementation, transdermal
291 patch, and topical vaginal cream (Lobo, 2017). Separating women by EHT modality, we observed
292 that women using oral and patch EHT had significant urobiome enrichment of *Lactobacillus* while
293 urobiome *Lactobacillus* enrichment varied widely in women using vaginal EHT (vEHT) and was
294 not significantly different from EHT(-) women (Figure 5A). We hypothesized that vEHT may differ
295 from oral and transdermal patch in composition, metabolism, or dosage. We therefore optimized
296 a published targeted liquid-chromatography mass spectrometry (LC-MS) method to quantify
297 excreted urinary estrogen conjugates of women in the No UTI History and rUTI Remission groups
298 (van der Berg et al., 2020). Limiting our analysis to the known major excreted sulfate and
299 glucuronide conjugates of estrone (E1) and 17β–estradiol (E2), we observed significantly higher
300 urinary concentrations of E1 and E2 sulfates and glucuronides in women using oral EHT. This
301 observation was concordant with urinary *Lactobacillus* abundance (Figure 5 B-D Figure S 6 A-D).
302 Women using patch EHT also exhibited high urinary *Lactobacillus* abundance and a significant
303 enrichment of urinary E1-sulfate compared to EHT(-) women (Figure S 5C). Consistent with
304 urinary *Lactobacillus* abundance, we observed no statistically significant difference in urinary
305 estrogen conjugate concentrations between vEHT(+) women and EHT(-) women (Figure 5 A-D
306 Figure S 6 A-D).

307 We further sought to determine if rUTI history differentially affected EHT-associated taxa by
308 dichotomizing patients by No UTI History and rUTI Remission group membership. We then
309 performed exploratory correlation analysis of creatinine-normalized estrogen metabolite
310 concentrations and the species-level taxonomic profile. We found a striking difference in estrogen-
311 associated taxonomic profiles between the No UTI History and rUTI Remission groups (Figure 5
312 E, F). We observed strong correlations between urinary E1 and E2 conjugates and *L. crispatus,*
313 *L. iners, and L. gasseri* in the No UTI History group, correlations which were not detected in the
314 rUTI Remission group (Figure 5 E, F Figure S 5 E, F). *B. breve*, an *Actinobacterium* associated
315 with colon health, exhibited the strongest positive correlation across estrogen conjugates in the
316 No UTI History group (Figure 5 E, G). This correlation was also absent in the urobiomes of the
317 rUTI Remission group. *A. prevotii* was consistently and significantly negatively associated with
318 urinary estrogens in the No UTI History group (Figure 5 E, Figure S 5 E). Fewer and distinct taxa
319 correlated with estrogen conjugates in the rUTI Remission group (Figure 5 F, Figure S 5F). It
320 should be noted that most EHT(+) women in the rUTI Remission group used vEHT (Figure 5 A).
321 To assess the robustness of these results, we used an independent, Bayesian correlation
322 approach to estimate normalized taxonomic abundances from read count-level data and account
323 for overdispersion (Tu, 2014). Consistent with the non-Bayesian analysis, *L. gasseri*, *B. dentium*,
324 *L. crispatus*, and *P. disiens* abundance were positively correlated with urinary estrogen conjugate
325 sum in the No UTI history group, while *A. prevotii* was negatively correlated. Bayesian analysis
326 also detected a set of new urinary estrogen-taxa correlations. Of note, *E. coli* was significantly
327 anti-correlated with summed urinary estrogen concentration in the No UTI History group and *R.*
328 *torques*, *Pantoea spp*., *Pseudomonas spp*., *Dorea spp*., and *C. aerofaciens* correlated with
329 estrogen in the rUTI Remission group (Figure 5 H). Conversely, *D. microaerophilus* and *C.*
330 *aurimucosum* were anti-correlated with urinary estrogen in the rUTI Remission group (Figure 5 I).
331 Together, these data indicate that distinct urinary taxa correlate with urinary estrogen metabolites
332 in women with No UTI history compared to women with rUTI history.
333
334 **Functional profiling reveals significant differences in the metabolic potential of cohort**
335 **urobiomes.**
336 We next sought to determine if rUTI leaves a detectable imprint on the functional metabolic
337 potential of the urobiome. We used the HUMAnN2 (v2.0) pipeline to profile the metabolic potential
338 encoded within cohort urobiomes (Franzosa et al., 2018). Principal component analysis (PCA)
339 performed on the relative abundance of encoded metabolic pathways in the three groups
340 identified discriminating clusters that separated the rUTI Relapse urobiomes from the rUTI

341 Remission and No UTI History urobiomes in the first two principal components (PCs) (Figure 6
342 A). These results were consistent with the taxonomic beta-diversity analysis (Figure 2 E). The
343 rUTI Relapse group ordinated along vectors defined by the enrichment of lipopolysaccharide
344 (LPS) biosynthesis (*n*=4 pathways), demethylmenaquinol-8 biosynthesis, fucose and mannose
345 degradation, D-galacturonate degradation, sucrose degradation, and the TCA cycle (Figure 6 B).
346 The rUTI Remission and No UTI History groups, which were not discriminated in the first two PCs,
347 ordinated along vectors defined by the enrichment of nucleotide biosynthesis (*n*=8 pathways), L-
348 lysine biosynthesis II, S-adenosyl methionine (SAM) biosynthesis, and UDP-N-acetyl-
349 glucosamine biosynthesis (Figure 6 B). These data suggest that the large-scale genetic potential
350 of the urobiome is relatively similar between rUTI Remission and No UTI History groups but is
351 dramatically altered during active rUTI.
352 Because dimensional reduction techniques often miss fine-scale discriminating features, we
353 next used LEfSe to identify metabolic pathway enrichments between the study groups (Segata et
354 al., 2011). First, we tested the hypothesis that rUTI history imparts functional changes on the
355 urobiomes of PM women by comparing the No UTI History and rUTI Remission groups. Forty-five
356 discriminatory metabolic pathways were significantly enriched in the rUTI Remission urobiomes
357 and four metabolic pathways significantly enriched in the No UTI History urobiomes with an FDR-
358 corrected $P<0.05$ and LDA >2 (Figure 6 C). The top 40 discriminating pathways were
359 carbohydrate metabolism (*n*=14), electron carrier biosynthesis (*n*=8), amino acid metabolism
360 (*n*=5), cell envelope biosynthesis (*n*=4), vitamin and cofactor biosynthesis (*n*=4), and
361 polysaccharide degradation (*n*=3) (Figure 6 C). While most of the discriminatory carbohydrate
362 metabolic pathways were enriched in the rUTI Remission urobiomes (13/14, 92.9%), we observed
363 an enrichment of D-galactose degradation (Leloir pathway) in the No UTI History group
364 (LDA=3.06, $P=0.028$). Conversely, electron carrier biosynthesis, namely biosynthetic pathways
365 for ubiquinol 7-10 as well as menaquinol 6, 9 and 10 and demethylmenaquinol 9, were strongly
366 enriched in the rUTI Remission urobiomes (Figure 6 C). L-lysine biosynthesis, L-threonine
367 biosynthesis, and L-tryptophan degradation were enriched in No UTI History urobiomes, while L-
368 ornithine biosynthesis and L-arginine degradation were enriched in rUTI Remission urobiomes.
369 The remaining discriminating metabolic pathways were enriched in the rUTI Remission urobiomes
370 and included cell envelope biosynthesis (e.g. LPS biosynthesis), vitamin metabolism (e.g.
371 coenzyme A biosynthesis), polysaccharide degradation (e.g. 4-deoxy L-threo hex-4-
372 enopyranuronate degradation), cinnamate and hydroxy cinnamate degradation, and ppGpp
373 biosynthesis (Figure 6 C). These data suggest that the metabolic landscape of the urobiome may
374 be significantly altered by rUTI history.

375 Pairwise differential enrichment analysis between the No UTI History and rUTI Relapse groups
376 identified 183 differentially enriched metabolic pathways (Figure 6 D). In line with the taxonomic
377 enrichment of Gram-negative species, we observed a strong enrichment of biosynthetic pathways
378 for lipopolysaccharide (LPS) within rUTI Relapse urobiomes. Top discriminating pathways
379 included carbohydrate (*n*=13), nucleotide (*n*=9), and amino acid metabolism (*n*=6), as well as cell
380 envelope biosynthesis (*n*=5) (Figure 6 D). We observed enrichment of diverse carbohydrate
381 degradation and central carbon metabolism pathways, including rhamnose, fucose, glyoxylate,
382 and fructuronate degradation in rUTI Relapse urobiomes (Figure 6 D). This was coupled with a
383 significant enrichment of TCA cycle metabolism, particularly 2-oxoglutarate decarboxylase and
384 ferroreductase (Figure 6 D). Only four metabolic pathways involved in carbohydrate metabolism,
385 including glycolysis from glucose and glucose 6-phosphate (G6P), pyruvate fermentation, and N-
386 acetyl glucosamine biosynthesis, were significantly differentially enriched in the No UTI History
387 urobiomes (Figure 6 D). Nucleic acid biosynthesis pathways were enriched in the No UTI History
388 group while the Relapsed rUTI group was enriched for nucleic acid degradation pathways (Figure
389 6 D). Differentially enriched amino acid metabolism pathways included L-lysine, L-threonine, and
390 L-isoleucine biosynthesis in the No UTI History group and L-phenylalanine biosynthesis in the
391 rUTI Relapse group (Figure 6 D). These results suggest that the urobiomes of the rUTI Relapse
392 group have the potential to utilize a more diverse nutrient set than the urobiomes of women who
393 do not experience UTI.
394
395 **Antibiotic resistance genes are enriched in the urobiomes of women with rUTI history**
396 Antibiotic therapy is currently the most prescribed treatment for the management of rUTI.
397 However, resistance to front-line antibiotics, such as TMP-SMX, fluoroquinolones, and
398 nitrofurantoin, is becoming a significant barrier to the successful treatment of rUTI (Malik et al.,
399 2018a). We used the GROOT resistome analysis pipeline to generate a detailed profile of the
400 antimicrobial resistance genes (ARGs) encoded within each urobiome (Rowe and Winn, 2018).
401 This analysis detected 55 high-confidence ARGs distributed among all three groups. We
402 observed significantly more ARGs in the urobiomes of the rUTI Remission (*P*=0.0455) and rUTI
403 Relapse (*P*=0.0302) groups compared to No UTI History urobiomes (Figure 7 A). Interestingly,
404 there was no significant difference in ARG count between rUTI Relapse and rUTI Remission
405 urobiomes. These data suggest that a history of rUTI leaves an imprint on the underlying
406 resistome of the urinary microbiota in PM women even in the absence of active infection.
407 To assess specific ARG enrichments associated with rUTI history, we performed differential
408 enrichment analysis using a Bayesian model of proportional enrichment (Jeffreys, 1946). The

409 TEM β-lactamase family, sulfonamide resistance genes *sul1* and *sul2*, and the *straA*
410 aminoglycoside 3'-phosphotransferase were significantly enriched in the rUTI Relapse group
411 while the aminoglycoside 3'-phosphotransferase genes, *aph(3')-III* and *aph(3')-Ia*, the macrolide
412 resistance gene, *ermB*, the β-lactam resistance gene *mecA*, and the aminoglycoside O-
413 nucleotidyltransferase gene, *ant(6)-Ia*, were enriched in the urobiomes of the rUTI Remission
414 group (Figure 7 B). Conversely, no ARGs were significantly enriched in the No UTI History group.
415 Identification of ARGs in metagenomes is only a prediction of the phenotype of a microbe or set
416 of microbes belonging to the sampled population (Quince et al., 2017). To begin to understand
417 how well metagenomic ARG analysis could predict phenotype, we measured antibiotic resistance
418 phenotypes of 22 unique bacterial uropathogens each isolated from an individual rUTI Relapse
419 patient. Species tested included *E. coli*, *K. pneumoniae*, *Klebsiella oxytoca*, *Streptococcus*
420 *anginosus*, *S. agalactiae*, *E. faecalis*, and *S. epidermidis*. Only 3 of the 15 strains with complete
421 or intermediate ampicillin resistance did not have a detected ampicillin resistance gene in the
422 associated metagenome (Figure 7 C). WGMS resistome profiling detected cefixime resistance
423 genes in 50% of the metagenomes (2/4) associated with isolates that were completely or
424 intermediately resistant to cefixime (Figure 7 C). Interestingly, the cefixime resistant strains
425 without a detected ARG were both streptococci. We observed that 50% of isolates exhibiting
426 resistance to TMP/SMX were isolated from urobiomes for which WGMS resistome profiling
427 detected the ARGs *sul I/II* and *drfA1* (Figure 7 C). In surveying aminoglycoside resistance, 50%
428 (1/2), 60% (3/5), 100% (1/1), 88.9% (8/9) of the isolates exhibiting complete or intermediate
429 resistance to Gentamicin, Kanamycin, Amikacin, and Streptomycin, respectively, were isolated
430 from urobiomes with detected corresponding ARGs (Figure 7 C). Metagenomic ARG analysis was
431 relatively poorly predictive for fluoroquinolone resistance with quinolone resistance genes
432 detected in only 27.3% (3/11) and 33.3% (2/6) of the associated metagenomes of isolates with
433 complete or intermediate resistance Ciprofloxacin and Levofloxacin, respectively (Figure 7 C).
434 This is likely because GROOT does not detect single nucleotide polymorphisms (SNPs) and
435 fluoroquinolone resistance is often conferred by SNPs in the genes encoding gyrase and
436 topoisomerase I (Correia et al., 2017). Relatively few urobiomes harbored resistance factors to
437 macrolides, which are not used in the treatment of Gram-negative infections (Arsic et al., 2018).
438 While all Gram-positive bacterial strains were resistant to erythromycin, macrolide ARGs were
439 only detected in the associated metagenomes of three strains. Tetracycline and phenicol ARGs
440 were respectively detected in 42.9% (3/7) and 0% (0/1) of the metagenomes associated with
441 strains with intermediate or resistant phenotypes (Figure 7C).
442

443 **Discussion**

444 A decade of research has identified and characterized the urobiome (Brubaker and Wolfe, 2017;
445 Hilt et al., 2014; Lewis et al., 2013; Price et al., 2019; Siddiqui et al., 2011; Wolfe et al., 2012). It
446 has become evident that the urobiome is involved in the progression of, or affected by, urinary
447 tract disease. Given the connection between host health and microbiome composition, the
448 urobiome has drawn significant attention in further understanding rUTI susceptibility. Most WGMS
449 studies of the female urobiome have been in younger or mixed age cohorts with little focused
450 representation of PM women, leaving critical gaps in our knowledge of a heavily impacted
451 demographic (Vaughan et al., 2021). Here, we present the first use of WGMS to specifically probe
452 urobiome ecology and function associated with rUTI in PM women. We found that bacteria make
453 up the majority of the non-human, non-viral metagenome of the PM urobiome and confirmed the
454 viability of 93.9% of the genera observed at >5% relative abundance in the WGMS data by
455 advanced urine culture. The main uropathogen detected in the rUTI Relapse group was UPEC,
456 while urobiomes of the No UTI History and rUTI Remission groups were either dominated by a
457 single bacterial species or were diverse. Both the No UTI History and rUTI Remission groups
458 exhibited subsets of women with urobiomes dominated by *L. crispatus, L. gasseri*, *L. iners*, *B.*
459 *breve*, *B. dentium*, *B. longum*, and *G. vaginalis*. These data support the observations by Thomas-
460 White et al. of an interconnected urogenital microbiome (Thomas-White et al., 2018). We detected
461 low abundances of fungal and archaeal taxa in all groups; however, little is known about the role
462 of fungi and archaea in the female urobiome.

463 We identified differentially enriched urobiome taxa between healthy PM women and those with
464 a history of rUTI that may serve as microbial biomarkers of urogenital tract health. Many of the
465 genera enriched in the rUTI Remission group, including *Peptoniphilus, Prevotella, Actinomyces,*
466 *Finegoldia, Fusobacterium,* and *Brevibacterium* were all members of the largest co-occurrence
467 network that clustered strongly around the genus, *Peptoniphilus,* a known member of the vaginal
468 microbiome associated with dysbiosis (Diop et al., 2019; Marrazzo et al., 2008; Onderdonk et al.,
469 2016). These data suggest that mutualistic relationships between *Peptoniphilus* and co-occurring
470 taxa may be key to defining community structure in urobiomes of women with increased rUTI
471 susceptibility (Faust et al., 2012). Conversely, while the genus *Lactobacillus* and the species *L.*
472 *vaginalis* and *L. crispatus* were enriched in No UTI History urobiomes, co-occurrence analysis
473 revealed a negative association between *Lactobacillus* and *Peptoniphilus* suggesting an
474 antagonistic relationship between the two genera. Taken together, these observations give new
475 insight into potentially biologically relevant interactions in the urobiome that may underlie rUTI
476 susceptibility. These observations are supported by a 2021 report by Vaughan et al. that used

477 16S rRNA amplicon sequencing to identify taxonomic differences between PM women with rUTI
478 and healthy controls and identified differences in the orders *Clostridiales* and *Prevotellaeceae,*
479 which, for example, contain the genera *Peptoniphilus* and *Prevotella,* respectively (Vaughan et
480 al., 2021). Critical questions for future research will be to validate signatures of urinary dysbiosis
481 associated with rUTI susceptibility in longitudinal studies.

482 Estrogen hormone therapy (EHT) is a common intervention to reduce discomfort associated
483 with menopause (Fait, 2019). EHT, especially vEHT, is also gaining prevalence as a rUTI
484 prophylactic in PM women because estrogen is thought to favor *Lactobacillus* colonization of the
485 vaginal and urinary microbiomes (Raz and Stamm, 1993; Stamm, 2007). Multiple independent
486 studies have evaluated associations between EHT and vaginal and urinary lactobacilli with
487 varying results (Anglim et al., 2021; Thomas-White et al., 2020). For example, Anglim et al. found
488 that vEHT did not significantly alter urinary lactobacilli populations among PM women with and
489 without rUTI while Thomas-White et al. reported that vEHT led to a significant enrichment of
490 urinary lactobacilli in PM women with overactive bladder symptoms (Anglim et al., 2021; Thomas-
491 White et al., 2020). In the present study, we identify *L. crispatus and L. vaginalis* as uniquely
492 associated with EHT use in PM women. Interestingly, streptococci as well as *A. vaginae*, a Gram-
493 positive species associated with *G. vaginalis* in bacterial vaginosis, were enriched in the
494 urobiomes of women not using EHT (Bradshaw et al., 2006). Importantly, careful analysis of
495 clinical metadata found a strong link between oral and patch EHT use, but not vEHT use, and the
496 presence of *Lactobacillus* in the urobiome. We hypothesized that EHT modalities may differ in
497 dosage, composition, patient compliance, or primary metabolism. 17β-estradiol was the active
498 ingredient in all oral and patch EHT formulations, but only 64.7% of vEHT(+) women used 17β-
499 estradiol cream. The remaining vEHT(+) women used conjugated estrogen creams. Our data
500 suggests that both oral and patch EHT are associated with elevated concentrations of urinary
501 estrogen conjugates, while vEHT was not. We further identified disease state-specific taxa-
502 estrogen metabolite correlations. *B. breve, L. iners*, *L. crispatus*, and *L. gasseri*, positively
503 correlated with urinary estrogen conjugate concentration in the No UTI history group but not the
504 rUTI Remission group. We hypothesize that this may be because rUTI Remission women were
505 predominantly taking vEHT or because rUTI history itself perturbs the underlying urobiome.
506 Future mechanistic research in relevant model systems and longitudinal human cohorts is needed
507 to define the effects of modality of and rUTI history on EHT urobiome modulation.

508 Frequent and repeated treatment of rUTI with antibiotics is thought to spur the evolution of
509 antibiotic resistance among uropathogenic bacteria and perhaps within the urobiome (Abbo and
510 Hooton, 2014; Malik et al., 2018a; Waller et al., 2018). Despite the urgent need to understand the

511 impact of antibiotic therapy on the urobiome, differences in urobiome ARG prevalence associated
512 with rUTI and rUTI history had not been previously investigated. We found that the urobiomes of
513 both the rUTI Relapse and rUTI Remission groups contained significantly more ARGs than the
514 No UTI History group suggesting that rUTI history may enrich for ARG-containing urobiomes. Of
515 note, rUTI Relapse urobiomes were enriched for β-lactam, aminoglycoside, and sulfonamide
516 resistance genes while rUTI Remission urobiomes were enriched for β-lactam, aminoglycoside,
517 macrolide resistance genes. Limitations of this analysis include that the analytical pipeline does
518 not distinguish between TEM alleles and does not detect common SNPs known to confer
519 fluoroquinolone resistance, for example.
520 Altogether, this work represents the first controlled WGMS analysis of urobiome structure and
521 function in PM women with different histories of rUTI and provides a robust foundation for further
522 mechanistic studies of the role of the urobiome in rUTI susceptibility and disease progression that
523 are necessary for the development of urobiome-aware alternative therapies for a rUTI.
524
525 **Methods**
526 **Patient Recruitment and Cohort Curation**
527 The current study is approved under IRBs STU032016-006 (University of Texas Southwestern
528 Medical Center) and 19MR0011 (University of Texas at Dallas). To estimate the number of
529 patients needed to enroll into each cohort group and predict statistical power, we performed a
530 series of power analyses using the 'pwr' package (https://github.com/heliosdrm/pwr) in the R-
531 statistical language based on ranging effect sizes from small to large for both multivariate analysis
532 of 3 groups with equal sample size and pairwise-based comparisons of two groups. Balancing
533 cost and clinical feasibility with predicted statistical power, we chose a sample size of 25 for each
534 cohort group. Patients were recruited from the Urology Clinic at the University of Texas
535 Southwestern Medical Center between April 2018 and October 2019. Written informed consent
536 was obtained from each patient prior to recruitment into the study cohorts. All patients were PM
537 females. The following set of exclusion criteria were used to initially screen patient's candidacy
538 for enrollment into the cohort: pre- or perimenopausal status; complicated rUTI; antibiotic
539 exposure within the 4 weeks prior to urine sample donation unless an active infection was
540 detected by culture; pelvic malignancy or history of pelvic radiation within 3 years before urine
541 sample donation; currently receiving chemotherapy; exhibiting renal insufficiency (creatinine >1.5
542 mg/dL); most recent post void residual (PVR) greater than 100 mL; greater than stage 2 prolapse;
543 pelvic procedure for incontinence within 6 months prior to urine sample donation; use of
544 intermittent catheterization; neurogenic bladder; any upper urinary tract abnormality which may

545 explain rUTI; and Diabetes Mellitus (DM) type 1 or 2. All urine samples were obtained by clean-
546 catch midstream urine collection and therefore were representative of the urogenital microbiome,
547 rather than specifically just the bladder microbiome. Patients were educated about the cleaning
548 and urine collection needs for this sampling technique prior to urine collection. Urine samples
549 were stored at 4°C for no more than 4 hours before sample processing, aliquoting, and biobanking
550 at -80°C. In total, 258 patients were recruited and screened for enrollment candidacy through
551 interview, clinical assessment, and electronic medical records
552 Patients were further vetted by self-reporting of UTI history, mining clinical history from
553 electronic patient records, clinical (standard) urine culture, and urine culture on Chromogenic agar
554 (BBL CHROMagar Orientation, BD). Clinical urine culture was performed on samples from all
555 patients with active UTI symptoms by the Clinical Microbiology Laboratory at UT Southwestern
556 Medical Center. Group assignment criteria were as follows. No UTI History: no self-reported or
557 clinical history of UTI, no UTI symptoms at the time of urine collection. rUTI Remission: recent
558 history of rUTI, no UTI symptoms at time of sample collection. rUTI Relapse: recent history of
559 rUTI, active UTI symptoms at time of urine collection, positive clinical urine culture. Positive urine
560 culture was defined as $>10^4$ bacterial CFU/mL.
561
562 **Advanced Urine Culture, Isolate Identification, and Isolate Biobanking**
563 Glycerol-stocked urine samples (stored at -80ºC) were thawed at room temperature, and then
564 diluted 1:3 and 1:30 in sterile 1X Phosphate Buffered Saline to adjust plating density for high and
565 low biomass samples. 100 µl of urine from each dilution was plated onto blood agar plates (BAP),
566 CHROMagar Orientation, De Man, Rogosa, and Sharpe (MRS) agar, Rabbit BAP (R-BAP), BD
567 BBL CDC anaerobe blood agar (CDC AN-BAP), and Columbia Colistin Naladixic Acid Agar
568 (CNA). Following plating, BAP was incubated in ambient and 5% CO_2 atmospheres, CHROMagar
569 Orientation in 5% CO_2, MRS and R-BAP in microaerophilic conditions, BD BBL CDC anaerobe
570 blood agar (CDC AN-BAP) in microaerophilic and anaerobic conditions and CNA in all four
571 atmospheric conditions. Plates were incubated at 35°C for 4 days in the respective atmosphere.
572 It should be noted that we were unable to culture *Gardnerella spp.* using these methods. However,
573 WGMS profiling frequently detected *G. vaginalis* in the sampled urobiomes. For targeted isolation
574 of *Gardnerella spp*.,100 µl urine was plated onto Human polysorbate-80 (HBT) bilayer medium in
575 microaerophilic atmosphere for 3 days. To isolate fungal species, 100 µl urine was plated onto
576 Brain Heart Infusion Agar supplemented with 20 g/L glucose and 50 mg/µl of chloramphenicol
577 (BHIg-Cam) and incubated at 5% CO2 for 3 days.

578 Bacterial identification was performed by PCR amplification and Sanger sequencing of the 16S
579 rRNA gene from well-isolated colonies as described previously (De Nisco et al., 2019). Briefly,
580 16S rRNA gene was amplified using primers 8F (5'-AGAGTTTGATCCTGGCTCAG-3') and
581 1492R (5'-GGTTACCTTGTTACGACTT-3') by colony PCR (Vaishnava et al., 2011) using
582 DreamTaq Master Mix (ThermoFisher Scientific) and 0.2μM primers. Amplicon size was
583 confirmed on 1% agarose gel, followed by gel purification (Bio basic) and Sanger Sequencing
584 (Genewiz) using the 8F primer. Sequences were analyzed using BLASTn against the NCBI 16S
585 ribosomal RNA (Bacteria and Archaea) database.
586 For fungal identification, ITS1 and ITS2 regions were amplified using the primer sequences
587 ITS1: 5'-TCCGTAGGTGAACCTGCGG-3' and ITS2: 5'-GCTGCGTTCTTCATCGATGC-3' from
588 well-isolated colonies and Sanger sequenced (Genewiz, South Plainfield, NJ, USA). Sequences
589 were analyzed using BLASTn against the NCBI ITS from Fungi type and reference material
590 database.
591 All the isolated and taxonomically identified isolates (*n*=896) were assigned a distinct ID and
592 biobanked at -80ºC in glycerol. The isolates were grown in Brain Heart Infusion broth, Tryptic Soy
593 Broth (BD 211825), MRS broth or NYCIII according to their growth preferences and stocked in
594 16% sterile glycerol for long-term storage at -80C.
595
596 **Metagenomic DNA Isolation, Library Construction, and Sequencing**
597 Prior to WGMS, we assessed the quality and reproducibility of 3 metagenomic DNA extraction
598 techniques: a modified genomic DNA (gDNA) isolation based on the Qiagen blood and tissue
599 DNAeasy Kit, the Zymo Research DNA/RNA microbiome miniprep, and a modified
600 phenol/chloroform/isoamyl alcohol extraction as demonstrated by Moustafa et al. (Moustafa et al.,
601 2018). After assessing the quality and yield of metagenomic DNA isolated using the three
602 methods, we chose the Zymo Research method. Urine samples were allowed to thaw on ice at
603 4°C. 10-20 mL of urine was centrifuged for 15 minutes at 4000 x g at 4°C. Urine pellets were
604 resuspended in 750 μL of DNA/RNA Shield (Zymo Research), transferred to a bead beating tube,
605 and subjected to ten 30 sec cycles of mechanical bead beating, with 5 min cooling between each
606 cycle. After mechanical lysis, the maximum volume of sample was collected and transferred to a
607 new microcentrifuge tube with DNA/RNA lysis buffer (Zymo). Nucleic acids were purified via the
608 Zymo Research DNA/RNA microbiome miniprep kit per the manufacturer's instruction. Elution of
609 DNA from the column was performed in nuclease-free water and each column was eluted twice
610 to maximize DNA recovery. As a control to internally assess gDNA extraction efficiency and
611 WGMS limit of detection (LOD), gDNA was concurrently extracted from commercially available

612 community standards (ZymoBiomics) using the same methods. gDNA was also extracted from
613 nuclease-free water to account for kit and environmental contamination. All DNA samples were
614 subjected to 16S rRNA gene amplification by PCR and visualized by agarose gel electrophoresis
615 to ensure microbial DNA was present before proceeding with WGMS. DNA yield and purity for all
616 samples were assessed by agarose gel electrophoresis, and by fluorescence-based Qubit
617 quantitation of DNA, RNA, and protein. Prior to library preparation the DNA concentration of each
618 sample was normalized and 20pg of spike-in gDNA was added (Zymo Research High Bacterial
619 Load Spike-in), which contains gDNA from the bacterial species *Imchella halotolerans* and
620 *Allobacillus halotolerans*, which are known to not be associated with humans.
621 WGMS was performed at the University of Texas at Dallas Genome Center using 2x150 bp
622 paired-end reads on a Illumina NextSeq 500. Library preparation was performed using Nextera
623 DNA Flex kit. Library preparation of the entire cohort and community standard and water controls
624 was distributed over 2 batches with overlapping samples. All samples were sequenced using
625 2x150 base pair paired-end sequencing in high output mode with a target of ≥50 million paired
626 end reads per sample.
627
628 **Bioinformatic Analyses**
629 All taxonomic, functional, and resistome bioinformatic analyses were performed on an in-house
630 Dell PowerEdge T630 server tower with 256GB RAM, 12 core Intel Xenon processor with 16TB
631 storage capacity or at the Texas Advanced Computing Center (TACC).
632 **Data Preprocessing**
633 The fastq files were checked for read quality, adapter content, GC contents, species
634 contamination using fastqc (v0.11.2) and fastq_screen (v0.4.4) (Andrews, 2015; Wingett and
635 Andrews, 2018). Low-quality reads (a quality score of less than Q20) and adapter were removed
636 using Trim galore (v 0.4.4) (Krueger) (Figure S 1D). Human DNA sequences were removed using
637 KneadData (Huttenhower). After host removal, the dataset contained an average of $2.6x10^7$ non-
638 human reads per sample.
639 **Taxonomic Profiling, Ecological Modeling, and Co-Occurrence Analysis**
640 The taxonomic assignment and estimation of composition of microbial species present in each
641 sample was performed using MetaPhlAn2 (Segata et al., 2012). MetaPhlAn2 estimates the
642 relative abundance of species by mapping the metagenomic reads against a clade specific marker
643 gene database. The database consists of bacterial, archaeal, viral and eukaryotic genomes. We
644 further used merge_metaphlan_tables module of MetaPhlAn2 to combine the relative abundance
645 estimates of samples in a cohort into one table.

646 To identify kit, environmental, and background contaminating taxonomic signals, we sequenced
647 a water sample which was randomly inserted into the metagenomic DNA preparation protocol.
648 Sequencing and taxonomic analysis of this sample revealed known kit and environmental
649 contaminants, such as *Delftia*, *Stenotrophomonas*, *Ralstonia*, *Bradyrizobium*, and others (Salter
650 et al., 2014). Unless a known member of the human microbiome, these taxa were censored. We
651 observed a small relative abundance of taxa salient to the human urobiome in the water control,
652 such as *Pseudomonas*, *Escherichia*, *Klebsiella*, *Enterococcus*, *Staphylococcus*, and
653 *Corynebacterium.* These signals ranged from 0.051%-11.5% of approximately 3 million mappable
654 reads observed in the water control (Figure S 2A). We further assessed the WGMS limit of reliable
655 detection using a commercially available log community standard (ZymoBiomics), which is
656 composed of multiple Gram-positive and Gram-negative bacterial and fungi. We observed a
657 strong linear correlation between the theoretical and observed relative abundance above 0.001%.
658 We therefore set a relative abundance threshold of 0.001% for a taxon to be considered as
659 detected within a sample (Figure S 1E). Species-level MetaPhlAn 2 taxonomic assignments were
660 not included in analysis if they were "unclassified".
661 Alpha-diversity analysis was performed at the species-level using phyloseq (version 1.16.2)
662 (McMurdie and Holmes, 2013). Beta-diversity analysis was performed using DPCoA on the
663 species-level taxonomic relative abundance dataset using phyloseq (version 1.16.2)(McMurdie
664 and Holmes, 2013). Taxonomic co-occurrence was performed with CCREPE pipeline using the
665 Pearson correlation and compositionally corrected P-values
666 (https://github.com/biobakery/biobakery/wiki/ccrepe#22-ccrepe-function). Network analysis of
667 taxonomic co-occurrences was performed using CytoScape (Version 3.8.2) with edges defined
668 by the correlation coefficients between taxa nodes in the default prefuse force directed layout.
669 **Taxonomic Correlation with Urinary Estrogens**
670 The Spearman correlation was calculated between a given taxa and urinary estrogen conjugate
671 or conjugate sum using the associate function from the regclass R package. To account for the
672 compositionality of the taxa when computing the correlations, the species-level taxonomic
673 composition dataset was transformed using the centered log ratio (CLR) transformation using the
674 clr function from the rgr R package. Nominal P-values were calculated by permutation. No multiple
675 hypothesis correction was performed on Nominal P-values as we considered this an exploratory
676 analysis (Althouse, 2016).
677 The Bayesian correlation analysis employed a posterior distribution with the Dirichlet-
678 Multinomial (DM) mode for the full data likelihood and a non-informative uniform prior proportional
679 to one (Tu, 2014). The DM models the non-transformed count data directly and estimates their

680 normalized abundances while accounting for overdispersion in the species-level count data. We
681 then computed the Spearman correlation between each of the estimated normalized abundances
682 and urinary estrogen conjugate sum. For posterior inference, we computed the 95% credible
683 intervals and posterior means for the correlation between each of the normalized abundances
684 and urinary estrogen conjugate sum. The correlation of a taxa-estrogen pair was significant if zero
685 was not contained in the credible interval. Further for the significant pairs, we calculated the ratio
686 of the proportion of posterior samples with correlations greater than 0.3 to those less than or equal
687 to 0.3. This ratio (Posterior Ratio) indicates correlation strength where a ratio higher than one
688 indicates a more moderate or strong correlation and less than one indicates a weak correlation.

689 **Functional Metabolic Profiling**

690 Functional metabolic profiling was performed using HUMAnN 2.0 (Franzosa et al., 2018).
691 HUMAnN2 uses a tiered approach to identify the functional profile of microbial communities.
692 Firstly, it maps the sample reads to clade specific markers and creates a database of pangenomes
693 for each sample. In the second tier, it performs the nucleotide level mapping of samples reads
694 against pangenome database. Lastly, a translated search against Uniref90 is performed for
695 unaligned reads in each sample (Suzek et al., 2015). The output result is the mapping of reads to
696 gene sequences with known taxonomy. The reads are normalized to gene sequence length to
697 give an estimate of per-organism and community total gene family abundance. Next, gene
698 families were analyzed to reconstruct and quantify metabolic pathways using MetaCyc (Caspi et
699 al., 2018). Different modules of HUMAnN such as humann2_join_table and
700 humann2_renorm_table were used to merge the pathway abundance of all the samples in a
701 cohort and normalize the abundance to counts per million (cpm) respectively. We filtered the
702 results to only include pathways whose taxonomic range included bacteria. We further censored
703 pathways which were specifically associated with a particular taxon due to database bias toward
704 commonly isolated and studied species. PCA of functional pathways was performed on the
705 pathway level relative abundance dataset using factroextra (https://cran.r-
706 project.org/web/packages/factoextra/readme/README.html). Pathway differential abundance
707 analysis was performed using LEfSe (Segata et al., 2011) on the pathway-level relative
708 abundance dataset. LEfSe uses Kruskal Wallis and Wilcoxon tests to find the differential
709 pathways between microbial communities. Finally, it uses LDA model to rank the pathways.

710 **Resistome Profiling and ARG Enrichment**

711 We used the GROOT (Graphing Resistance Out Of meTagenomes) to generate a profile of
712 antimicrobial resistance genes within the urobiomes of the present study (Rowe and Winn, 2018).
713 The default database ARG-ANNOT was used for alignment of the metagenomics reads.

714 Subsequently GROOT report command was used to generate a profile of antibiotic resistance
715 genes at a read coverage of 90%. Filtering of the GROOT results was performed to insure high
716 confidence in ARG presence within the urobiomes. We used a cutoff of a sufficient amount of
717 reads to generate 10x coverage of an ARG to qualify its detection within a urobiome. We further
718 collapsed alleles of the β-lactamase genes TEM, CTX, OXA, OXY2, SHV, and *cfxA* as well as the
719 aminoglycoside ARG Aac3-IIa and Aac3-IIe alleles into single gene-level features to account for
720 multiple-mapping reads.

721 Bayesian modeling of the resistome data was performed as follows. Resistome data for the
722 three cohorts (Never = 1, Remission = 2, Relapse = 3) consisted of 186 antimicrobial resistance
723 genes (ARG) which were collapsed into family-level genes ($G = 55$). Each cell in the data set
724 contained a binary indicator of no detection (0) or detection (1) of the resistance family-level gene
725 within each patient sample such that $x_{gik} = \{0,1\}, g = 1, \cdots, 55, i = 1, \cdots, 25, k = 1,2,3$ indicates no
726 detection or detection of resistance family-level gene g respectively for sample i in cohort k.

727 A Bayesian Beta-Bernoulli model with Jeffreys prior was used to model the posterior
728 distributions of group proportions and pairwise differences for the g family-level genes. Two
729 posterior inferences were performed. First, we removed any family-level genes that had no
730 significant pairwise contrast of cohort proportions using 95% credible intervals as criteria. We
731 determined that a significant family level-gene does not have zero contained in a 95% credible
732 interval for at least one pairwise contrast. Second, we computed the posterior probability and
733 Bayes Factor (BF) to make inferences on each pairwise contrast of cohort proportions of only the
734 significant family-level genes. The posterior probability of a particular contrast was computed as
735 the proportion of posterior samples satisfying that contrast. The BF computed for each contrast
736 represented the odds of H_1: "at least one cohort's proportion (ω) for gene g is different" in favor of
737 $H_0: \omega_{g1} = \omega_{g2} = \omega_{g3}$.

738 **Taxonomic Biomarker Analysis**

739 We applied two methods of taxonomic differential abundance analysis employing the robust and
740 widely used LEfSe pipeline as well as BMDA, a recently described Bayesian model of differential
741 abundance (Li et al., 2019). LEfSe analysis was performed as previously described (Segata et
742 al., 2011). For the BMDA model we first applied the quality control step (detailed in the supplement
743 of Li et al., 2019) to the raw count data. We then fitted the BMDA model, which is a Bayesian
744 hierarchical framework that uses a zero-inflated binomial model to model the raw count data and
745 a Gaussian mixture model with feature selection to identify differentially abundant taxa. The
746 BMDA can fully account for zero-inflation, over-dispersion, and varying sequencing depth. We
747 chose weakly informative priors on all parameters of the model to avoid biased results. For model

748 fitting and posterior inference, BMDA implements the Metropolis-Hastings algorithm within a
749 Gibbs sampler. The marginal posterior probability of inclusion (PPI) was used to identify the set
750 of discriminating taxa between the control and disease groups. Marginal PPI is the proportion of
751 MCMC samples in which a taxon is selected to be discriminatory if it is greater than a pre-specified
752 value. We chose a threshold such that the expected Bayesian false discovery rate (FDR) was
753 less than 0.05.
754
755 **Antibiotic susceptibility testing**
756 Assessment of antibiotic (abx) susceptibility was performed via the Kirby-Bauer disk diffusion
757 susceptibility test (Hudzicki, 2009). Antibiotic disks were prepared by aliquoting 10uL of antibiotic
758 stock (GEN 1mg/ml, AMP 1mg/ml, CIP 0.5mg/ml, LVX 0.5mg/ml, ERM 1.5mg/ml, CHL 3mg/ml,
759 TMP/SMX 1.25/23.75mg/ml, NIT 30mg/ml, DOX 3mg/ml) onto the disk in a sterile petri dish and
760 drying at room temperature in the dark. Vehicle control disks were prepared similarly using the
761 diluents of each antibiotic. Strains were streaked from frozen glycerol stocks onto CHROMagar
762 or Blood Agar (species dependent) and incubated overnight at 37ºC in ambient conditions or 35ºC
763 in 5% CO2. Single, well-isolated colonies were inoculated into 3 mL Brain-Heart-Infusion broth
764 and incubated at the respective atmospheric conditions for 16 – 18 hours. After incubation,
765 cultures were normalized to 0.5 McFarland standard, washed, and resuspended in sterile 1X
766 Phosphate-Buffered Saline (PBS). 150 μL of standardized culture were pipetted onto 150 mm
767 Mueller-Hinton Agar plates and spread using sterile glass beads. Plates were dried in sterile
768 conditions before abx-impregnated disks were placed on the surface of the agar. *E. coli* strain
769 ATCC25922 was used for quality and vehicle controls. Sterile 1X PBS was plated as sterility
770 control. Plates were incubated inverted per the recommendations of Clinical and Laboratory
771 Standards Institute (CLSI) M100-ED30: 2020 Performance Standards for Antimicrobial
772 Susceptibility Testing, 30th Edition
773 (https://clsi.org/standards/products/microbiology/documents/m100/). After incubation,
774 antimicrobial susceptibility was evaluated by measurement of the zone of inhibition and using
775 CLSI established zone diameter breakpoints.
776
777 **Liquid Chromatography Mass Spectrometry Measurement of Estrogen Metabolites**
778 Direct measurement of urinary estrogen metabolites was performed via a modification of
779 previously reported methods(van der Berg et al., 2020). Briefly, urine (500 μL) was diluted and
780 spiked with 100 ng stable isotope-labeled internal standards of d3-Estrone 3-Glucuronide and d4-
781 Estradiol 3-Sulfate. Diluted and spiked samples were loaded onto an equilibrated Phenomenex

782 C18 cartridge for solid phase extraction to separate conjugated estrogens. Following aqueous
783 methanolic extraction of estrogen conjugates and non-polar extraction of free estrogens with
784 methanolic acetone, fractions were dried by vacuum centrifugation and prepared for LC-MS/MS
785 analysis. Estrogen conjugates (sulfates and glucuronides) were directly assayed using a curated
786 and optimized MRM library by LC-MS/MS.
787 High sensitivity quantitative LC-MS/MS was performed on a Waters Xevo TQ tandem
788 quadrupole MS lined to an ACQUITY UPLC with a Selectra C8 RP column (100x2.1 mm 1.8μm,
789 UCT). MRM libraries of estrogen conjugates have been curated to include both analytical and
790 confirmatory transitions for each analyte at optimal retention times to maximize separation. Briefly,
791 data analysis was performed by integrating the peak area of the analytical transition for each
792 analyte. Peak areas were normalized to molecular class-matched internal spike-in standards and
793 mapped to a standard curve to accurately estimate analyte concentration. Urine estrogen
794 metabolite concentrations were then normalized to urinary creatinine, which was measured by
795 colorimetric assay (Sigma).
796
797 **Statistical Analysis**
798 Statistical analysis was performed using R statistical programing, GraphPad Prism 9, and
799 Microsoft Excel. For hypothesis testing, non-parametric Mann-Whitney U-test was used for
800 pairwise comparisons and the Kruskal-Wallis non-parametric ANOVA with multiple comparison
801 post-hoc was used for non-paired and unmatched comparisons of 3 or more groups. Multiple
802 comparison adjustment was performed using false discover rate (FDR) when appropriate. An
803 alpha of 0.05 was used to control type I error.
804
805 **Acknowledgements**
806 We wish to acknowledge and sincerely thank the patients who participated in this study. This
807 work was supported by a research grant from The Welch Foundation, a research grant from the
808 Foundation for Women's Wellness, NIH grant 1R01DK131267-01, and The University of Texas
809 at Dallas Startup funds to NJD, the Cecil H. and Ida Green Chair in Systems Biology Science to
810 KLP, The Felicia and John Cain Distinguished Chair in Women's Health to PZ. We would also
811 like to thank all the members of the De Nisco and Palmer labs for their helpful and creative input
812 throughout this study. We would further like to acknowledge and thank the Genome Center at the
813 University of Texas at Dallas for their invaluable work and assistance in generating the
814 metagenomic dataset used for this study.
815

816 **Author Contributions**

817 Conceptualization, M.L.N., P.E.Z., K.L.P., N.J.D.; data curation, M.L.N., J.F., A.Kup., A.P.A.;
818 formal analysis, M.L.N, A.Kumar., K.C.L., C.Z., Q.L., C.X., V.S., N.J.D.; funding acquisition, V.S.,
819 K.L.P, P.E.Z., N.J.D.; investigation, M.L.N., N.V.H., V.H.N., A.N.; methodology, M.L.N., A.Kumar.,
820 N.V.H., K.C.L., V.H.N., A.N., B.M.S., Q.L., C.X., V.S., P.E.Z., K.L.P., N.J.D.; project
821 administration, M.L.N., P.E.Z., N.J.D.; resources, P.E.Z., K.L.P., N.J.D.; software, M.L.N.,
822 A.Kumar., K.C.L., C.Z., Q.L., C.X.; supervision, Q.L., C.X., V.S., P.E.Z., K.L.P., N.J.D; validation,
823 M.L.N., N.V.H., K.C.L., C.Z.; visualization, M.L.N., V.H.N.; writing-original draft, M.L.N., A.K.,
824 N.V.H., K.C.L., Q.L., C.X., N.J.D.

825

826 **Supplemental materials**

827 Table S1. Cohort clinical characteristics

828 Figure S1. Power analysis and metagenomic dataset characteristics.

829 Figure S2. WGMS environmental contaminants and patient-level urine culturing coverage

830 Figure S3. Taxonomic profiles of detected *Archea, Eukaryota*, and Vial species.

831 Figure S4. Ecological modeling indices among the cohort groups.

832 Figure S5. Urinary estrogen conjugate concentrations and taxonomic associations.

833

834 **Figure legends**

835 **Figure 1. Study design and summary of genera detected by WGMS and advanced urine**
836 **culture.** (A) Illustration of rUTI cycle depicting periods of active, symptomatic UTI with positive
837 urine culture followed by periods of remission with negative urine culture. (B) Diagram of cohort
838 structure and datasets generated for the study created with BioRender.com. (C) Taxonomic
839 cladogram of top 20 genera detected in all metagenomes (*n*=75) by Metaphlan2. Node size
840 indicates relative abundance and branch length is arbitrary. (D) Venn diagram depicting the
841 coverage of advanced urine culture calculated at the genus level considering all bacterial genera
842 with >5% WGMS relative abundance in at least one patient.

843

844 **Figure 2. The bacterial taxonomic profile of rUTI in PM women.** Genus (A) and species-level
845 (B) taxonomic profiles of the top 15 bacterial genera among cohort groups (No UTI History (*n*=25),
846 rUTI Remission (*n*=25), rUTI Relapse (*n*=25)). Remaining genera or species are combined into
847 "Other". Alpha-diversity comparison of observed species counts (C) and Shannon index (D)
848 between groups (1 = No UTI History, 2 = rUTI Remission, 3 = rUTI Relapse). Solid lines represent
849 medians while dotted lines represent the interquartile range. *P*-value generated by Kruskal-Wallis

850 test with Dunn's multiple correction post hoc. (E) Beta-diversity of the WGMS data by DPCoA.
851 Each dot represents an individual sample color-coded by group (No UTI history in blue, rUTI
852 remission in purple, and rUTI relapse in salmon). Vectors (grey) represent major discriminating
853 loadings (*i.e.* species). (F) Volcano plot depicting co-occurrence of genera within the WGMS
854 dataset by Pearson correlation. *P*-value generated by permutation. Red dots represent
855 associations with an FDR-corrected *P*-value < 0.05. Blue dots represent associations with a
856 nominal *P*-value < 0.05, but an FDR-corrected *P*-value > 0.05. (G) Network analysis of all genus-
857 level co-occurrences with nominal *P*-value < 0.05. Nodes represent genera. Edges are defined
858 by Pearson correlation and node size is proportional to the degree, or connectivity, of the node.
859
860 **Figure 3. Bayesian modeling detects the taxonomic imprint of rUTI history on the urobiome**
861 **of PM women.** Bayesian differential abundance model comparing genus (A) and species-level
862 (B) taxonomic enrichment between the No UTI history (*n*=25) and rUTI Remission (*n*=25) groups.
863 Dots, indicating the $\log_{10}$(posterior effect size), are color-coded by group enrichment (No UTI
864 history in blue and rUTI Remission in purple). Lines indicate the 95% credible interval and PPI
865 denotes posterior probability index.
866
867 **Figure 4. Estrogen hormone therapy shapes the urobiome of PM women.**
868 Genus (A) and species-level (B) taxonomic profiles of the relative abundance of the top 22
869 bacterial genera among EHT(-) (*n*=21) and EHT(+) (*n*=29) women in the No UTI History and rUTI
870 Remission groups. All genera or species not within the top 22 are combined into "Other". (C)
871 Comparison of *Lactobacillus* relative abundance between EHT(-) (grey) and EHT(+) (pink) women
872 in the No UTI history and rUTI Remission groups. Observed species count (D), Shannon index
873 (E), and Simpson index (F) comparisons between EHT(-) (grey) and EHT(+) (pink) women in the
874 No UTI history and rUTI remission groups. Violin plots depict the smoothed distribution of the
875 data. Solid lines represent medians while dotted lines represent the interquartile range. *P*-values
876 generated by Wilcoxon rank-sum. (G) Two significantly differentially enriched genera (LDA > 4.5)
877 detected by LEfSe between EHT(-) (grey) and EHT(+) (pink) women. LDA denotes the $\log_{10}$(linear
878 discriminant analysis score) and the *P*-value was generated by LEfSe. (H) Differentially enriched
879 taxa between EHT(-) (grey) and EHT(+) (pink) women in the No UTI history and rUTI Remission
880 cohorts detected by BMDA. Dots indicate $\log_{10}$(posterior effect size) and PPI denotes posterior
881 probability index. S. m/o/p denotes *Streptococcus mitus/oralis/pneumoniae*.
882

883 **Figure 5. Distinct taxa-urinary estrogen metabolite associations between PM women with**
884 **and without rUTI history.** (A) Comparison of the relative *Lactobacillus* abundance between
885 EHT(-) (grey, *n*=21) and EHT(+) (pink, *n*=29) women separated by EHT modality (Oral, Patch,
886 Vaginal). Creatinine (Cr)-normalized summed estrogen conjugates (B), E1 conjugates (C) and E2
887 conjugates (D) measured in No UTI History and rUTI Remission urine separated by EHT modality
888 (EHT(-) (n=20), Oral (*n*=6), Patch (*n*=6), Vaginal (*n*=17)). For all box and whisker plots, error bars
889 are drawn from minimum to maximum, boxes represent interquartile range, solid lines denote the
890 median, and *P*-value generated by Kruskal-Wallis test with Dunn's multiple correction post hoc.
891 Spearman correlation of bacterial species with summed Cr-normalized urinary estrogen
892 conjugates in No UTI History (E) and rUTI remission (F) groups. *P*-value generated by
893 permutation. Red and blue dots represent significant ($p<0.05$) positive and negative associations,
894 respectively. (G) Correlation scatter plots of *B. breve*, *L. iners*, *L. crispatus*, and *A. prevotti,* and
895 summed Cr-normalized urinary estrogen conjugate associations among No UTI History (*n*=25)
896 (blue) and rUTI Remission women (*n*=23) (purple). Linear regression trend line (solid line) is
897 shown with 95% confidence intervals. Bayesian correlation point estimates and 95% credible
898 interval of posterior correlation (Spearman) for the top 10 taxa and Cr-normalized summed urinary
899 estrogen conjugates in the (H) No UTI History and (I) rUTI Remission groups. Blue indicates
900 negative while red indicates positive correlation. Significant correlations also found in the non-
901 Bayesian analysis are bolded.
902
903 **Figure 6. rUTI history and active infection shape the metabolic potential of the urobiome.**
904 (A, B) PCA of cohort urobiomes by metagenome-encoded metabolic pathways. Depiction of
905 ordination and clustering in the first two PCs in (A) and vectors (grey) defining major discriminatory
906 loadings (*i.e.* metabolic pathways) in (B). Top 40 differentially enriched pathways between No UTI
907 history (blue) and rUTI Remission (purple) groups (C) and the No UTI history and rUTI Relapse
908 (red) groups (D) detected by LEfSe. Pathways met an FDR-corrected *P*-value cutoff of < 0.05.
909 LDA indicates $\log_{10}$(linear discriminant analysis).
910
911 **Figure 7. rUTI history and active infection shape the resistome of the PM urobiome.** (A)
912 Comparison of the ARGs detected within the urobiomes of the No UTI History, rUTI Remission,
913 and rUTI Relapse groups. Violin plot depicts the smoothed distribution of the data. Solid lines
914 represent median while dotted lines represent interquartile range. *P*-value generated by Kruskal-
915 Wallis test with uncorrected Dunn's multiple correction post hoc. (B) Bayesian differential
916 enrichment analysis of ARGs within cohort urobiomes. Group comparisons were determined by

917 pairwise differences in ARG(+) proportions. 95% credible intervals, Bayes factor, and posterior
918 probability are presented for interpretation. Fisher exact *P*-values are also provided. (C)
919 Agreement between urobiome ARG detection and antibiotic resistance phenotypes of isolates of
920 the most abundant species present in each rUTI Relapse patient (*E. coli* (*n*=15), *Klebsiella* (*n*=3),
921 *Streptococcus* (*n*=3), *E. faecalis* (*n*=1), *S. epidermidis* (*n*=1)). Upper diagonal colors represent
922 WGMS profiling results (blue = ARG (+), white = ARG(-)). Lower diagonal color represents isolate
923 phenotype (red = resistant, yellow = intermediate resistance, white = sensitive, grey = not tested).
924

925 **References**

926 Abbo, L.M., and Hooton, T.M. (2014). Antimicrobial Stewardship and Urinary Tract Infections.
927 Antibiotics (Basel) *3*, 174-192.

928 Alteri, C.J., Himpsl, S.D., and Mobley, H.L. (2015). Preferential use of central metabolism in vivo
929 reveals a nutritional basis for polymicrobial infection. PLoS Pathog *11*, e1004601.

930 Althouse, A.D. (2016). Adjust for Multiple Comparisons? It's Not That Simple. Ann Thorac Surg
931 *101*, 1644-1645.

932 Ammitzboll, N., Bau, B.P.J., Bundgaard-Nielsen, C., Villadsen, A.B., Jensen, A.M., Leutscher,
933 P.D.C., Glavind, K., Hagstrom, S., Arenholt, L.T.S., and Sorensen, S. (2021). Pre- and
934 postmenopausal women have different core urinary microbiota. Sci Rep *11*, 2212.

935 Andrews, S. (2015). FastQC: a quality control tool for high throughput sequence data.

936 Anglim, B., Phillips, C., Shynlova, O., and Alarab, M. (2021). The effect of local estrogen therapy
937 on the urinary microbiome composition of postmenopausal women with and without recurrent
938 urinary tract infections. Int Urogynecol J.

939 Arsic, B., Barber, J., Cikos, A., Mladenovic, M., Stankovic, N., and Novak, P. (2018). 16-membered
940 macrolide antibiotics: a review. Int J Antimicrob Agents *51*, 283-298.

941 Barraud, O., Ravry, C., Francois, B., Daix, T., Ploy, M.C., and Vignon, P. (2019). Shotgun
942 metagenomics for microbiome and resistome detection in septic patients with urinary tract
943 infections. Int J Antimicrob Agents.

944 Bradshaw, C.S., Tabrizi, S.N., Fairley, C.K., Morton, A.N., Rudland, E., and Garland, S.M. (2006).
945 The association of Atopobium vaginae and Gardnerella vaginalis with bacterial vaginosis and
946 recurrence after oral metronidazole therapy. J Infect Dis *194*, 828-836.

947 Brubaker, L., and Wolfe, A.J. (2017). The female urinary microbiota, urinary health and common
948 urinary disorders. Ann Transl Med *5*, 34.

949 Bucevic Popovic, V., Situm, M., Chow, C.T., Chan, L.S., Roje, B., and Terzic, J. (2018). The urinary
950 microbiome associated with bladder cancer. Sci Rep *8*, 12157.

951 Caspi, R., Billington, R., Fulcher, C.A., Keseler, I.M., Kothari, A., Krummenacker, M., Latendresse,
952 M., Midford, P.E., Ong, Q., Ong, W.K.*, et al.* (2018). The MetaCyc database of metabolic pathways
953 and enzymes. Nucleic Acids Res *46*, D633-D639.

954 Ceccarani, C., Foschi, C., Parolin, C., D'Antuono, A., Gaspari, V., Consolandi, C., Laghi, L., Camboni,
955 T., Vitali, B., Severgnini, M.*, et al.* (2019). Diversity of vaginal microbiome and metabolome during
956 genital infections. Sci Rep *9*, 14095.

957 Correia, S., Poeta, P., Hebraud, M., Capelo, J.L., and Igrejas, G. (2017). Mechanisms of quinolone
958 action and resistance: where do we stand? J Med Microbiol *66*, 551-559.

959 De Nisco, N.J., Neugent, M., Mull, J., Chen, L., Kuprasertkul, A., de Souza Santos, M., Palmer, K.L.,
960 Zimmern, P., and Orth, K. (2019). Direct Detection of Tissue-Resident Bacteria and Chronic
961 Inflammation in the Bladder Wall of Postmenopausal Women with Recurrent Urinary Tract
962 Infection. J Mol Biol *431*, 4368-4379.

963 Diop, K., Diop, A., Michelle, C., Richez, M., Rathored, J., Bretelle, F., Fournier, P.E., and Fenollar,
964 F. (2019). Description of three new Peptoniphilus species cultured in the vaginal fluid of a woman
965 diagnosed with bacterial vaginosis: Peptoniphilus pacaensis sp. nov., Peptoniphilus raoultii sp.
966 nov., and Peptoniphilus vaginalis sp. nov. Microbiologyopen *8*, e00661.

967 Edwards, V.L., Smith, S.B., McComb, E.J., Tamarelle, J., Ma, B., Humphrys, M.S., Gajer, P.,
968 Gwilliam, K., Schaefer, A.M., Lai, S.K.*, et al.* (2019). The Cervicovaginal Microbiota-Host
969 Interaction Modulates Chlamydia trachomatis Infection. MBio *10*.

970 Fait, T. (2019). Menopause hormone therapy: latest developments and clinical practice. Drugs
971 Context *8*, 212551.

972 Faust, K., Sathirapongsasuti, J.F., Izard, J., Segata, N., Gevers, D., Raes, J., and Huttenhower, C.
973 (2012). Microbial co-occurrence relationships in the human microbiome. PLoS Comput Biol *8*,
974 e1002606.

975 Flores-Mireles, A.L., Walker, J.N., Caparon, M., and Hultgren, S.J. (2015). Urinary tract infections:
976 epidemiology, mechanisms of infection and treatment options. Nat Rev Microbiol *13*, 269-284.

977 Franzosa, E.A., McIver, L.J., Rahnavard, G., Thompson, L.R., Schirmer, M., Weingart, G., Lipson,
978 K.S., Knight, R., Caporaso, J.G., Segata, N.*, et al.* (2018). Species-level functional profiling of
979 metagenomes and metatranscriptomes. Nat Methods *15*, 962-968.

980 Gaitonde, S., Malik, R.D., and Zimmern, P.E. (2019). Financial Burden of Recurrent Urinary Tract
981 Infections in Women: A Time-driven Activity-based Cost Analysis. Urology *128*, 47-54.

982 Hardy, L., Jespers, V., Abdellati, S., De Baetselier, I., Mwambarangwe, L., Musengamana, V., van
983 de Wijgert, J., Vaneechoutte, M., and Crucitti, T. (2016). A fruitful alliance: the synergy between
984 Atopobium vaginae and Gardnerella vaginalis in bacterial vaginosis-associated biofilm. Sex
985 Transm Infect *92*, 487-491.

986 Hardy, L., Jespers, V., Dahchour, N., Mwambarangwe, L., Musengamana, V., Vaneechoutte, M.,
987 and Crucitti, T. (2015). Unravelling the Bacterial Vaginosis-Associated Biofilm: A Multiplex
988 Gardnerella vaginalis and Atopobium vaginae Fluorescence In Situ Hybridization Assay Using
989 Peptide Nucleic Acid Probes. PLoS One *10*, e0136658.

990 Hilt, E.E., McKinley, K., Pearce, M.M., Rosenfeld, A.B., Zilliox, M.J., Mueller, E.R., Brubaker, L., Gai,
991 X., Wolfe, A.J., and Schreckenberger, P.C. (2014). Urine is not sterile: use of enhanced urine
992 culture techniques to detect resident bacterial flora in the adult female bladder. J Clin Microbiol
993 *52*, 871-876.

994 Hudzicki, J. (2009). Kirby-Bauer disk diffusion susceptibility test protocol.

995 Huttenhower, C. KneadData.

996 Jeffreys, H. (1946). An invariant form for the prior probability in estimation problems. Proc R Soc
997 Lond A Math Phys Sci *186*, 453-461.

998 Jhang, J.F., and Kuo, H.C. (2017). Recent advances in recurrent urinary tract infection from
999 pathogenesis and biomarkers to prevention. Ci Ji Yi Xue Za Zhi *29*, 131-137.

1000 Karstens, L., Asquith, M., Caruso, V., Rosenbaum, J.T., Fair, D.A., Braun, J., Gregory, W.T., Nardos,
1001 R., and McWeeney, S.K. (2018). Community profiling of the urinary microbiota: considerations
1002 for low-biomass samples. Nat Rev Urol *15*, 735-749.

1003 Karstens, L., Asquith, M., Davin, S., Stauffer, P., Fair, D., Gregory, W.T., Rosenbaum, J.T.,
1004 McWeeney, S.K., and Nardos, R. (2016). Does the Urinary Microbiome Play a Role in Urgency
1005 Urinary Incontinence and Its Severity? Front Cell Infect Microbiol *6*, 78.

1006 Keogh, D., Tay, W.H., Ho, Y.Y., Dale, J.L., Chen, S., Umashankar, S., Williams, R.B.H., Chen, S.L.,
1007 Dunny, G.M., and Kline, K.A. (2016). Enterococcal Metabolite Cues Facilitate Interspecies Niche
1008 Modulation and Polymicrobial Infection. Cell Host Microbe *20*, 493-503.

1009 Kononen, E., and Wade, W.G. (2015). Actinomyces and related organisms in human infections.
1010 Clin Microbiol Rev *28*, 419-442.

1011 Krueger, F. Trim Galore!

1012 Lewis, D.A., Brown, R., Williams, J., White, P., Jacobson, S.K., Marchesi, J.R., and Drake, M.J.
1013 (2013). The human urinary microbiome; bacterial DNA in voided urine of asymptomatic adults.
1014 Front Cell Infect Microbiol *3*, 41.

1015 Li, Q., Jiang, S., Koh, A.Y., Xiao, G., and Zhan, X. (2019). Bayesian Modeling of Microbiome Data
1016 for Differential Abundance Analysis, pp. arXiv:1902.08741.

1017 Lobo, R.A. (2017). Hormone-replacement therapy: current thinking. Nat Rev Endocrinol *13*, 220-
1018 231.

1019 Malik, R.D., Wu, Y.R., Christie, A.L., Alhalabi, F., and Zimmern, P.E. (2018a). Impact of Allergy and
1020 Resistance on Antibiotic Selection for Recurrent Urinary Tract Infections in Older Women.
1021 Urology *113*, 26-33.

1022 Malik, R.D., Wu, Y.R., and Zimmern, P.E. (2018b). Definition of Recurrent Urinary Tract Infections
1023 in Women: Which One to Adopt? Female Pelvic Med Reconstr Surg *24*, 424-429.

1024 Marrazzo, J.M., Thomas, K.K., Fiedler, T.L., Ringwood, K., and Fredricks, D.N. (2008). Relationship
1025 of specific vaginal bacteria and bacterial vaginosis treatment failure in women who have sex with
1026 women. Ann Intern Med *149*, 20-28.

1027 McMurdie, P.J., and Holmes, S. (2013). phyloseq: an R package for reproducible interactive
1028 analysis and graphics of microbiome census data. PLoS One *8*, e61217.

1029 Moustafa, A., Li, W., Singh, H., Moncera, K.J., Torralba, M.G., Yu, Y., Manuel, O., Biggs, W., Venter,
1030 J.C., Nelson, K.E*., et al.* (2018). Microbial metagenome of urinary tract infection. Sci Rep *8*, 4333.

1031 Neugent, M.L., Hulyalkar, N.V., Nguyen, V.H., Zimmern, P.E., and De Nisco, N.J. (2020). Advances
1032 in Understanding the Human Urinary Microbiome and Its Potential Role in Urinary Tract Infection.
1033 mBio *11*.

1034 Onderdonk, A.B., Delaney, M.L., and Fichorova, R.N. (2016). The Human Microbiome during
1035 Bacterial Vaginosis. Clin Microbiol Rev *29*, 223-238.

1036 Pavoine, S., Dufour, A.B., and Chessel, D. (2004). From dissimilarities among species to
1037 dissimilarities among communities: a double principal coordinate analysis. J Theor Biol *228*, 523-
1038 537.

1039 Pearce, M.M., Hilt, E.E., Rosenfeld, A.B., Zilliox, M.J., Thomas-White, K., Fok, C., Kliethermes, S.,
1040 Schreckenberger, P.C., Brubaker, L., Gai, X*., et al.* (2014). The female urinary microbiome: a
1041 comparison of women with and without urgency urinary incontinence. MBio *5*, e01283-01214.

1042 Price, T.K., Dune, T., Hilt, E.E., Thomas-White, K.J., Kliethermes, S., Brincat, C., Brubaker, L., Wolfe,
1043 A.J., Mueller, E.R., and Schreckenberger, P.C. (2016). The Clinical Urine Culture: Enhanced
1044 Techniques Improve Detection of Clinically Relevant Microorganisms. J Clin Microbiol *54*, 1216-
1045 1222.

1046 Price, T.K., Hilt, E.E., Thomas-White, K., Mueller, E.R., Wolfe, A.J., and Brubaker, L. (2019). The
1047 urobiome of continent adult women: a cross-sectional study. BJOG.

1048 Quince, C., Walker, A.W., Simpson, J.T., Loman, N.J., and Segata, N. (2017). Shotgun
1049 metagenomics, from sampling to analysis. Nat Biotechnol *35*, 833-844.

1050 Ravel, J., and Brotman, R.M. (2016). Translating the vaginal microbiome: gaps and challenges.
1051 Genome Med *8*, 35.

1052 Ravel, J., Gajer, P., Abdo, Z., Schneider, G.M., Koenig, S.S., McCulle, S.L., Karlebach, S., Gorle, R.,
1053 Russell, J., Tacket, C.O.*, et al.* (2011). Vaginal microbiome of reproductive-age women. Proc Natl
1054 Acad Sci U S A *108 Suppl 1*, 4680-4687.

1055 Raz, R., and Stamm, W.E. (1993). A controlled trial of intravaginal estriol in postmenopausal
1056 women with recurrent urinary tract infections. N Engl J Med *329*, 753-756.

1057 Rowe, W.P.M., and Winn, M.D. (2018). Indexed variation graphs for efficient and accurate
1058 resistome profiling. Bioinformatics *34*, 3601-3608.

1059 Salter, S.J., Cox, M.J., Turek, E.M., Calus, S.T., Cookson, W.O., Moffatt, M.F., Turner, P., Parkhill,
1060 J., Loman, N.J., and Walker, A.W. (2014). Reagent and laboratory contamination can critically
1061 impact sequence-based microbiome analyses. BMC Biol *12*, 87.

1062 Segata, N., Izard, J., Waldron, L., Gevers, D., Miropolsky, L., Garrett, W.S., and Huttenhower, C.
1063 (2011). Metagenomic biomarker discovery and explanation. Genome Biol *12*, R60.

1064 Segata, N., Waldron, L., Ballarini, A., Narasimhan, V., Jousson, O., and Huttenhower, C. (2012).
1065 Metagenomic microbial community profiling using unique clade-specific marker genes. Nat
1066 Methods *9*, 811-814.

1067 Shipitsyna, E., Roos, A., Datcu, R., Hallen, A., Fredlund, H., Jensen, J.S., Engstrand, L., and Unemo,
1068 M. (2013). Composition of the vaginal microbiota in women of reproductive age--sensitive and
1069 specific molecular diagnosis of bacterial vaginosis is possible? PLoS One *8*, e60670.

1070 Siddiqui, H., Nederbragt, A.J., Lagesen, K., Jeansson, S.L., and Jakobsen, K.S. (2011). Assessing
1071 diversity of the female urine microbiota by high throughput sequencing of 16S rDNA amplicons.
1072 BMC Microbiol *11*, 244.

1073 Stamm, W.E. (2007). Estrogens and urinary-tract infection. J Infect Dis *195*, 623-624.

1074 Stamm, W.E., and Norrby, S.R. (2001). Urinary tract infections: disease panorama and challenges.
1075 J Infect Dis *183 Suppl 1*, S1-4.

1076 Stapleton, A.E., Au-Yeung, M., Hooton, T.M., Fredricks, D.N., Roberts, P.L., Czaja, C.A., Yarova-
1077 Yarovaya, Y., Fiedler, T., Cox, M., and Stamm, W.E. (2011). Randomized, placebo-controlled phase
1078 2 trial of a Lactobacillus crispatus probiotic given intravaginally for prevention of recurrent
1079 urinary tract infection. Clin Infect Dis *52*, 1212-1217.

1080 Suzek, B.E., Wang, Y., Huang, H., McGarvey, P.B., Wu, C.H., and UniProt, C. (2015). UniRef
1081 clusters: a comprehensive and scalable alternative for improving sequence similarity searches.
1082 Bioinformatics *31*, 926-932.

1083 Thomas-White, K., Forster, S.C., Kumar, N., Van Kuiken, M., Putonti, C., Stares, M.D., Hilt, E.E.,
1084 Price, T.K., Wolfe, A.J., and Lawley, T.D. (2018). Culturing of female bladder bacteria reveals an
1085 interconnected urogenital microbiota. Nat Commun *9*, 1557.

1086 Thomas-White, K., Taege, S., Limeira, R., Brincat, C., Joyce, C., Hilt, E.E., Mac-Daniel, L., Radek,
1087 K.A., Brubaker, L., Mueller, E.R.*, et al.* (2020). Vaginal estrogen therapy is associated with
1088 increased Lactobacillus in the urine of postmenopausal women with overactive bladder
1089 symptoms. Am J Obstet Gynecol *223*, 727 e721-727 e711.

1090 Thomas-White, K.J., Kliethermes, S., Rickey, L., Lukacz, E.S., Richter, H.E., Moalli, P., Zimmern, P.,
1091 Norton, P., Kusek, J.W., Wolfe, A.J.*, et al.* (2017). Evaluation of the urinary microbiota of women
1092 with uncomplicated stress urinary incontinence. Am J Obstet Gynecol *216*, 55 e51-55 e16.

1093 Tu, S. (2014). The Dirichlet-Multinomial and Dirichlet-Categorical models for Bayesian inference.

1094 Vaishnava, S., Yamamoto, M., Severson, K.M., Ruhn, K.A., Yu, X., Koren, O., Ley, R., Wakeland,
1095 E.K., and Hooper, L.V. (2011). The antibacterial lectin RegIIIgamma promotes the spatial
1096 segregation of microbiota and host in the intestine. Science *334*, 255-258.

1097 van der Berg, C.L., Venter, G., van der Westhuizen, F.H., and Erasmus, E. (2020). Data on the
1098 optimisation of a solid phase extraction method for fractionating estrogen metabolites from
1099 small urine volumes. Data Brief *29*, 105222.

1100 Vaughan, M.H., Mao, J., Karstens, L.A., Ma, L., Amundsen, C.L., Schmader, K.E., and Siddiqui, N.Y.
1101 (2021). The Urinary Microbiome in Postmenopausal Women with Recurrent Urinary Tract
1102 Infections. J Urol *206*, 1222-1231.

1103 Waller, T.A., Pantin, S.A.L., Yenior, A.L., and Pujalte, G.G.A. (2018). Urinary Tract Infection
1104 Antibiotic Resistance in the United States. Prim Care *45*, 455-466.

1105 Wingett, S.W., and Andrews, S. (2018). FastQ Screen: A tool for multi-genome mapping and
1106 quality control. F1000Res *7*, 1338.

1107 Wolfe, A.J., and Brubaker, L. (2019). Urobiome updates: advances in urinary microbiome
1108 research. Nat Rev Urol *16*, 73-74.

1109 Wolfe, A.J., Toh, E., Shibata, N., Rong, R., Kenton, K., Fitzgerald, M., Mueller, E.R.,
1110 Schreckenberger, P., Dong, Q., Nelson, D.E.*, et al.* (2012). Evidence of uncultivated bacteria in the
1111 adult female bladder. J Clin Microbiol *50*, 1376-1383.
1112

Figure 1

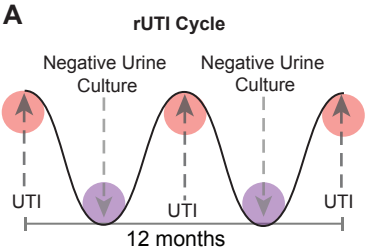
A
rUTI Cycle
Negative Urine Culture
Negative Urine Culture
UTI
UTI
UTI
12 months

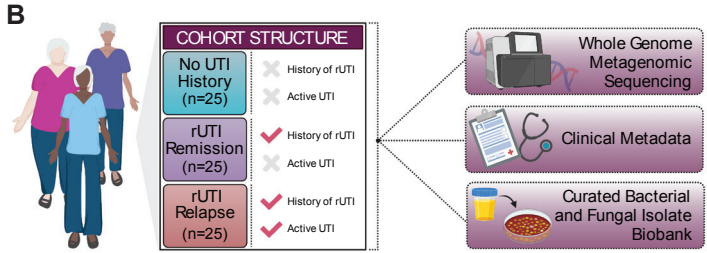
B
COHORT STRUCTURE
No UTI History (n=25)
History of rUTI
Active UTI
rUTI Remission (n=25)
History of rUTI
Active UTI
rUTI Relapse (n=25)
History of rUTI
Active UTI
Whole Genome Metagenomic Sequencing
Clinical Metadata
Curated Bacterial and Fungal Isolate Biobank

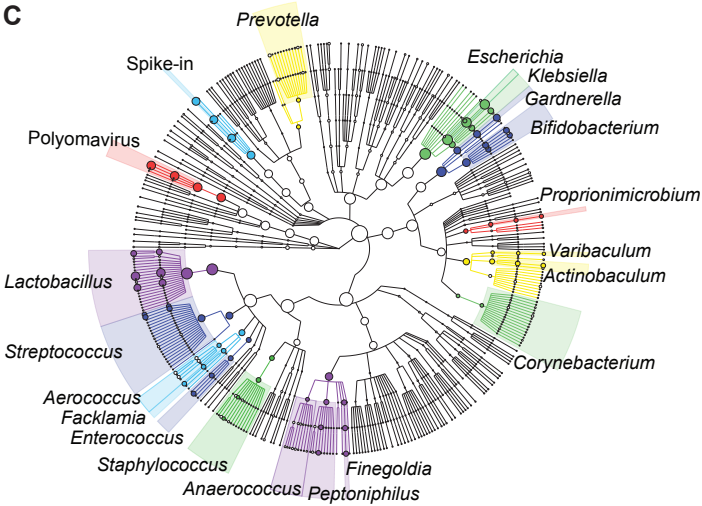
C
Prevotella
Spike-in
Escherichia
Klebsiella
Gardnerella
Polyomavirus
Bifidobacterium
Proprionimicrobium
Varibaculum
Actinobaculum
Lactobacillus
Streptococcus
Corynebacterium
Aerococcus
Facklamia
Enterococcus
Staphylococcus
Finegoldia
Anaerococcus
Peptoniphilus

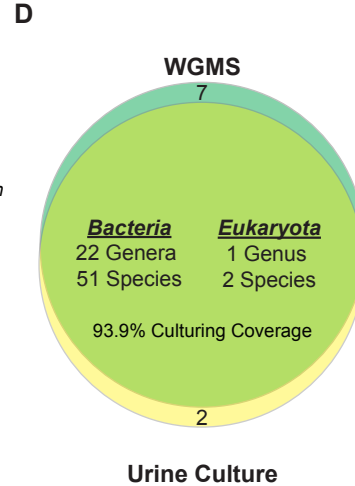
D
WGMS
7
Bacteria
22 Genera
51 Species
Eukaryota
1 Genus
2 Species
93.9% Culturing Coverage
2
Urine Culture

Figure 2

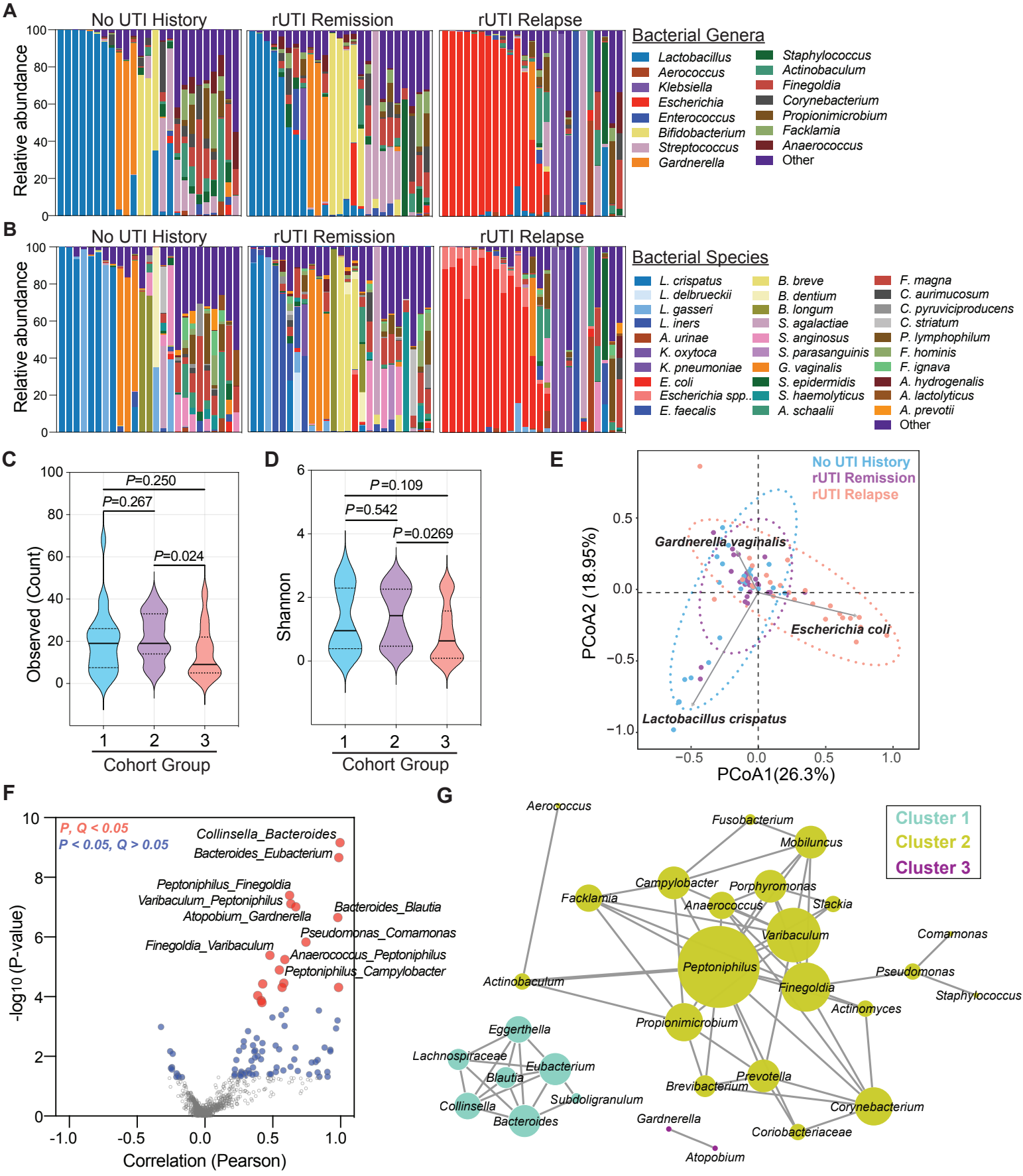
A
No UTI History
rUTI Remission
rUTI Relapse
Relative abundance
Bacterial Genera
Lactobacillus
Aerococcus
Klebsiella
Escherichia
Enterococcus
Bifidobacterium
Streptococcus
Gardnerella
Staphylococcus
Actinobaculum
Finegoldia
Corynebacterium
Propionimicrobium
Facklamia
Anaerococcus
Other
B
Bacterial Species
L. crispatus
L. delbrueckii
L. gasseri
L. iners
A. urinae
K. oxytoca
K. pneumoniae
E. coli
Escherichia spp..
E. faecalis
B. breve
B. dentium
B. longum
S. agalactiae
S. anginosus
S. parasanguinis
G. vaginalis
S. epidermidis
S. haemolyticus
A. schaalii
F. magna
C. aurimucosum
C. pyruviciproducens
C. striatum
P. lymphophilum
F. hominis
F. ignava
A. hydrogenalis
A. lactolyticus
A. prevotii
Other
C
Observed (Count)
P=0.250
P=0.267
P=0.024
Cohort Group
D
Shannon
P=0.109
P=0.542
P=0.0269
Cohort Group
E
No UTI History
rUTI Remission
rUTI Relapse
Gardnerella vaginalis
Escherichia coli
Lactobacillus crispatus
PCoA2 (18.95%)
PCoA1(26.3%)
F
P, Q < 0.05
P < 0.05, Q > 0.05
Collinsella_Bacteroides
Bacteroides_Eubacterium
Peptoniphilus_Finegoldia
Varibaculum_Peptoniphilus
Atopobium_Gardnerella
Bacteroides_Blautia
Pseudomonas_Comamonas
Finegoldia_Varibaculum
Anaerococcus_Peptoniphilus
Peptoniphilus_Campylobacter
-log10 (P-value)
Correlation (Pearson)
G
Cluster 1
Cluster 2
Cluster 3
Aerococcus
Fusobacterium
Mobiluncus
Campylobacter
Porphyromonas
Facklamia
Anaerococcus
Slackia
Varibaculum
Comamonas
Peptoniphilus
Pseudomonas
Actinobaculum
Finegoldia
Staphylococcus
Actinomyces
Propionimicrobium
Eggerthella
Lachnospiraceae
Eubacterium
Blautia
Prevotella
Brevibacterium
Subdoligranulum
Collinsella
Corynebacterium
Bacteroides
Gardnerella
Coriobacteriaceae
Atopobium

Figure 3

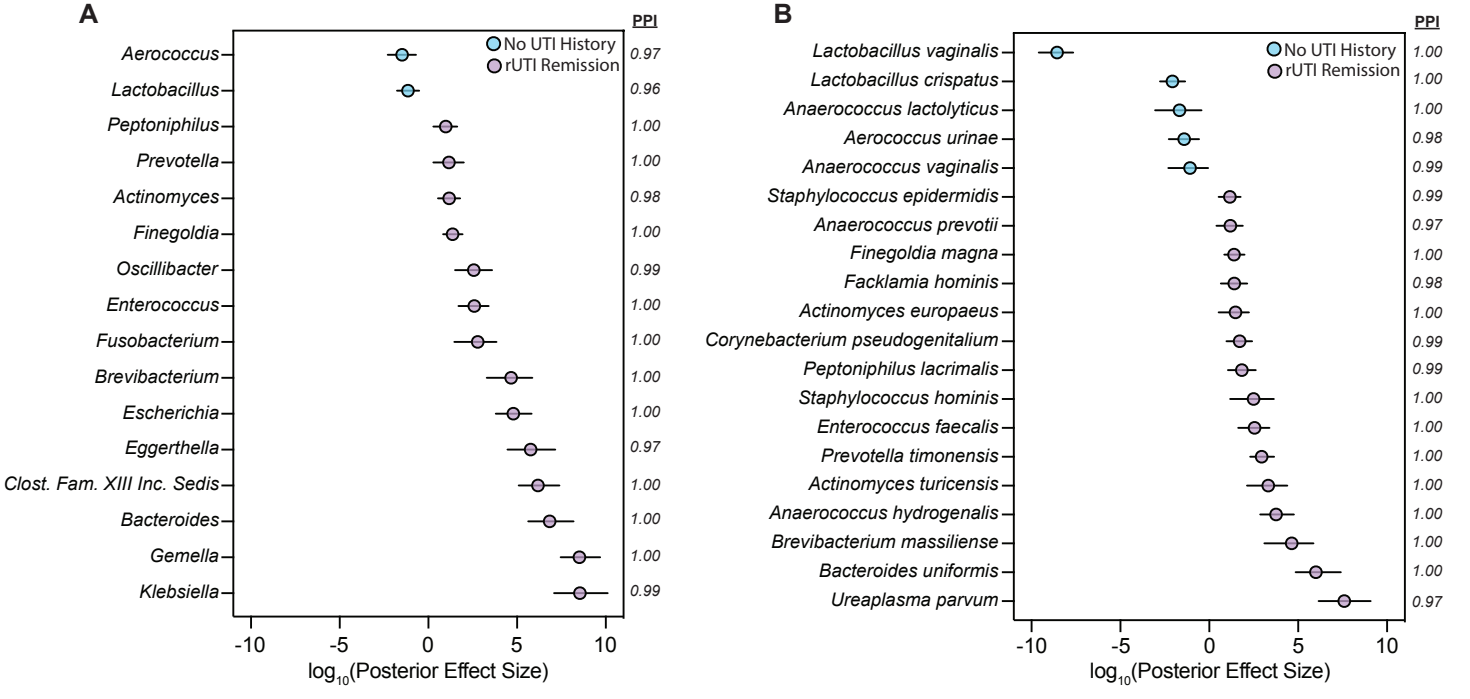
A
PPI
No UTI History
rUTI Remission
Aerococcus 0.97
Lactobacillus 0.96
Peptoniphilus 1.00
Prevotella 1.00
Actinomyces 0.98
Finegoldia 1.00
Oscillibacter 0.99
Enterococcus 1.00
Fusobacterium 1.00
Brevibacterium 1.00
Escherichia 1.00
Eggerthella 0.97
Clost. Fam. XIII Inc. Sedis 1.00
Bacteroides 1.00
Gemella 1.00
Klebsiella 0.99
-10 -5 0 5 10
log10(Posterior Effect Size)
B
PPI
No UTI History
rUTI Remission
Lactobacillus vaginalis 1.00
Lactobacillus crispatus 1.00
Anaerococcus lactolyticus 1.00
Aerococcus urinae 0.98
Anaerococcus vaginalis 0.99
Staphylococcus epidermidis 0.99
Anaerococcus prevotii 0.97
Finegoldia magna 1.00
Facklamia hominis 0.98
Actinomyces europaeus 1.00
Corynebacterium pseudogenitalium 0.99
Peptoniphilus lacrimalis 0.99
Staphylococcus hominis 1.00
Enterococcus faecalis 1.00
Prevotella timonensis 1.00
Actinomyces turicensis 1.00
Anaerococcus hydrogenalis 1.00
Brevibacterium massiliense 1.00
Bacteroides uniformis 1.00
Ureaplasma parvum 0.97
-10 -5 0 5 10
log10(Posterior Effect Size)

Figure 4

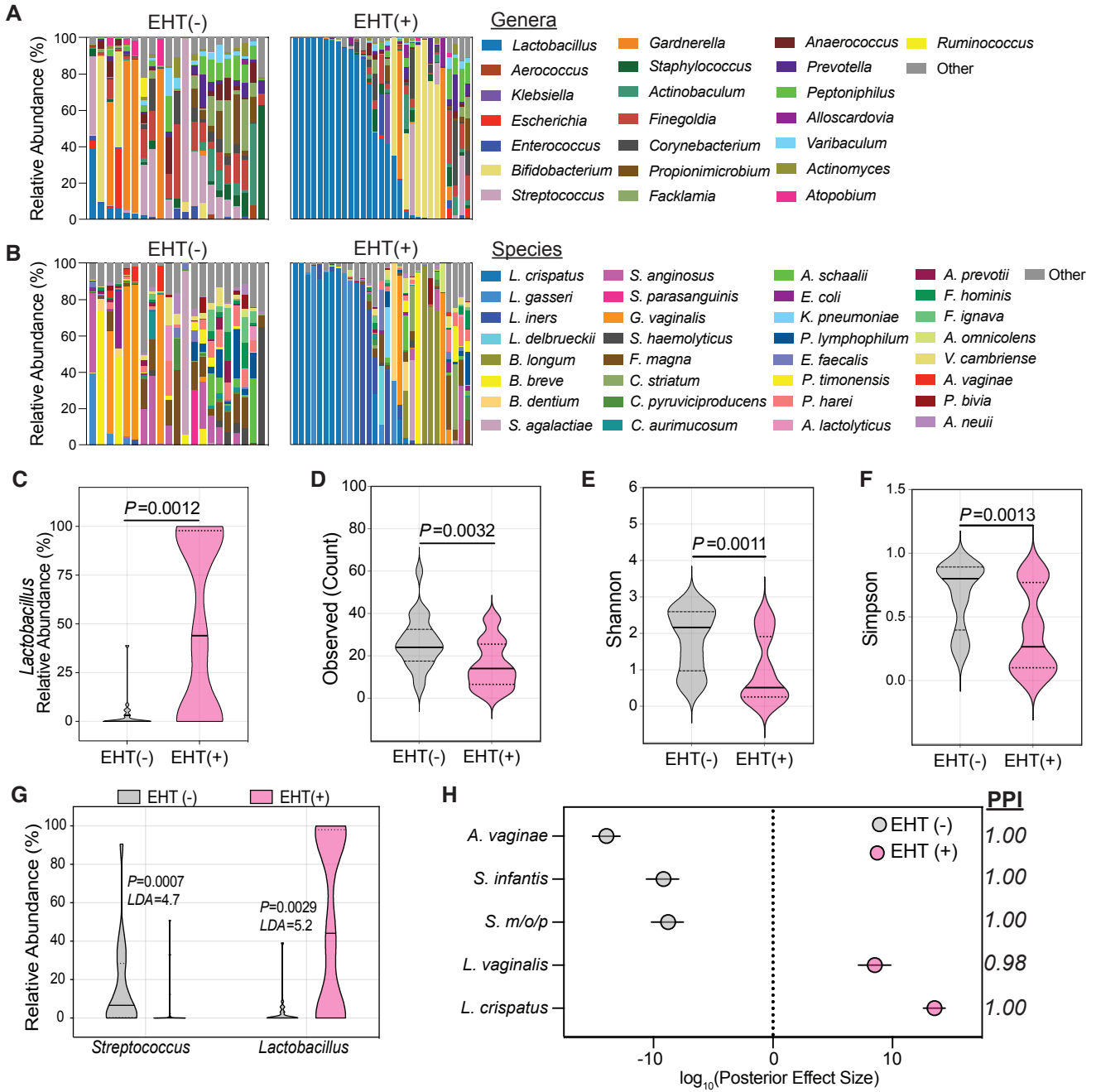
A
EHT(-)
EHT(+)
Relative Abundance (%)
Genera
Lactobacillus
Aerococcus
Klebsiella
Escherichia
Enterococcus
Bifidobacterium
Streptococcus
Gardnerella
Staphylococcus
Actinobaculum
Finegoldia
Corynebacterium
Propionimicrobium
Facklamia
Anaerococcus
Prevotella
Peptoniphilus
Alloscardovia
Varibaculum
Actinomyces
Atopobium
Ruminococcus
Other
B
Species
L. crispatus
L. gasseri
L. iners
L. delbrueckii
B. longum
B. breve
B. dentium
S. agalactiae
S. anginosus
S. parasanguinis
G. vaginalis
S. haemolyticus
F. magna
C. striatum
C. pyruviciproducens
C. aurimucosum
A. schaalii
E. coli
K. pneumoniae
P. lymphophilum
E. faecalis
P. timonensis
P. harei
A. lactolyticus
A. prevotii
F. hominis
F. ignava
A. omnicolens
V. cambriense
A. vaginae
P. bivia
A. neuii
Other
C
P=0.0012
Lactobacillus Relative Abundance (%)
D
P=0.0032
Observed (Count)
E
P=0.0011
Shannon
F
P=0.0013
Simpson
G
EHT (-)
EHT(+)
P=0.0007
LDA=4.7
P=0.0029
LDA=5.2
Streptococcus
Lactobacillus
H
PPI
A. vaginae 1.00
S. infantis 1.00
S. m/o/p 1.00
L. vaginalis 0.98
L. crispatus 1.00
log10(Posterior Effect Size)

Figure 5

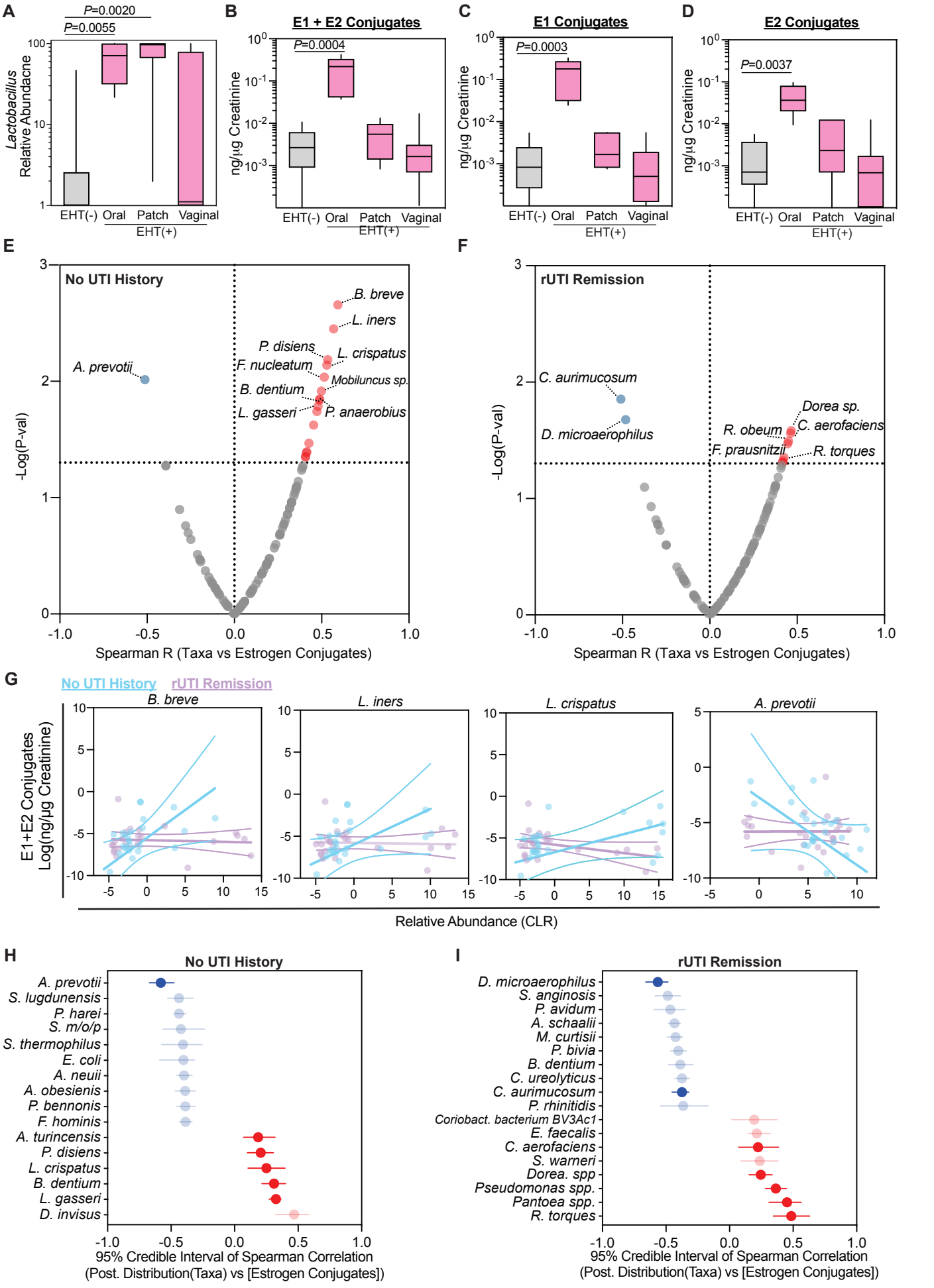
A
P=0.0020
P=0.0055
Lactobacillus Relative Abundance
EHT(-) Oral Patch Vaginal
EHT(+)
B
E1 + E2 Conjugates
P=0.0004
ng/µg Creatinine
C
E1 Conjugates
P=0.0003
D
E2 Conjugates
P=0.0037
E
No UTI History
B. breve
L. iners
P. disiens
L. crispatus
F. nucleatum
Mobiluncus sp.
B. dentium
L. gasseri
P. anaerobius
A. prevotii
-Log(P-val)
Spearman R (Taxa vs Estrogen Conjugates)
F
rUTI Remission
C. aurimucosum
D. microaerophilus
Dorea sp.
R. obeum
C. aerofaciens
F. prausnitzii
R. torques
G
No UTI History
rUTI Remission
B. breve
L. iners
L. crispatus
A. prevotii
E1+E2 Conjugates Log(ng/µg Creatinine)
Relative Abundance (CLR)
H
No UTI History
A. prevotii
S. lugdunensis
P. harei
S. m/o/p
S. thermophilus
E. coli
A. neuii
A. obesienis
P. bennonis
F. hominis
A. turincensis
P. disiens
L. crispatus
B. dentium
L. gasseri
D. invisus
95% Credible Interval of Spearman Correlation
(Post. Distribution(Taxa) vs [Estrogen Conjugates])
I
rUTI Remission
D. microaerophilus
S. anginosis
P. avidum
A. schaalii
M. curtisii
P. bivia
B. dentium
C. ureolyticus
C. aurimucosum
P. rhinitidis
Coriobact. bacterium BV3Ac1
E. faecalis
C. aerofaciens
S. warneri
Dorea. spp
Pseudomonas spp.
Pantoea spp.
R. torques
95% Credible Interval of Spearman Correlation
(Post. Distribution(Taxa) vs [Estrogen Conjugates])

Figure 6

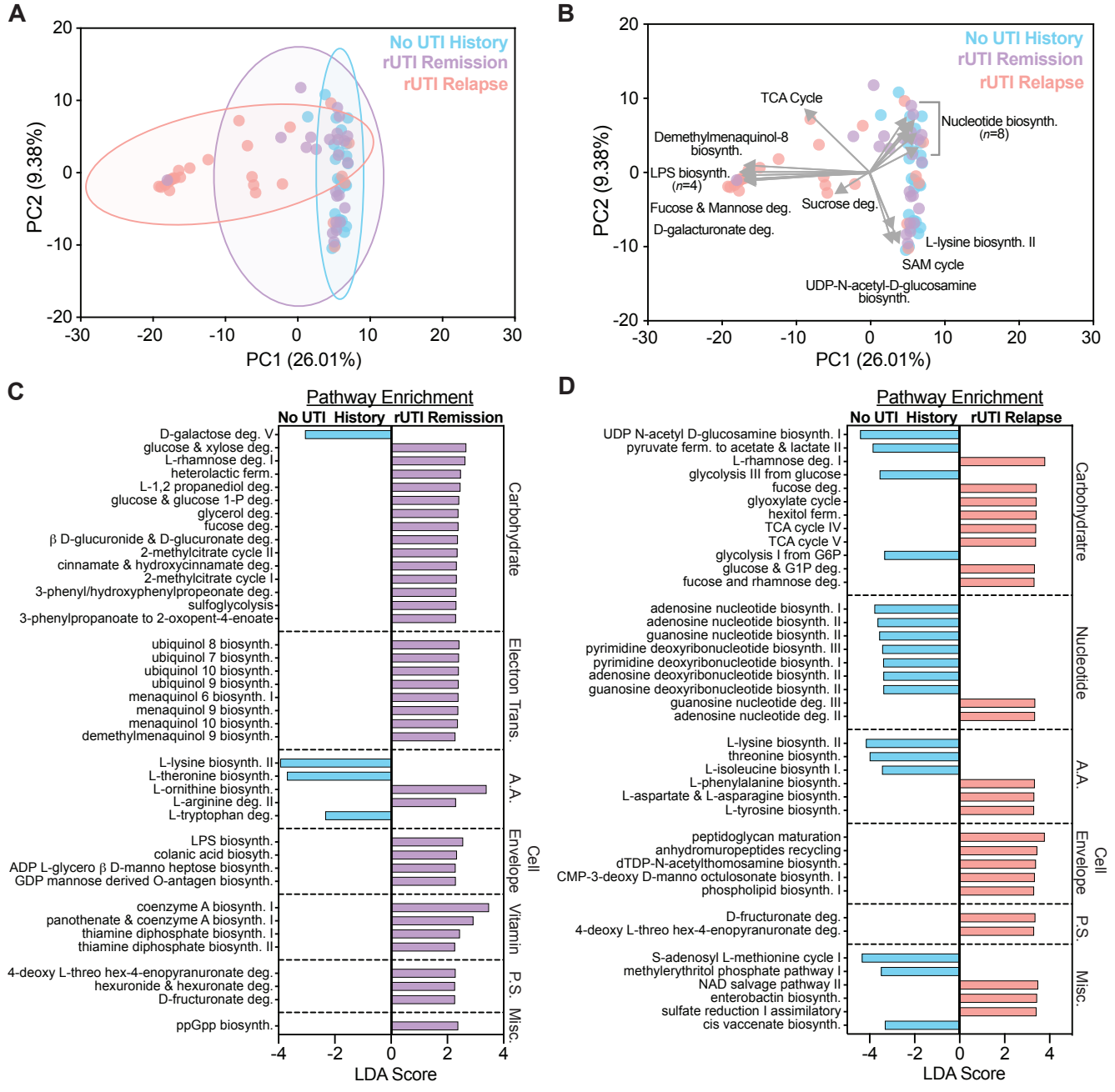
A
No UTI History
rUTI Remission
rUTI Relapse
PC2 (9.38%)
PC1 (26.01%)
B
No UTI History
rUTI Remission
rUTI Relapse
TCA Cycle
Nucleotide biosynth. (n=8)
Demethylmenaquinol-8 biosynth.
LPS biosynth. (n=4)
Fucose & Mannose deg.
Sucrose deg.
D-galacturonate deg.
L-lysine biosynth. II
SAM cycle
UDP-N-acetyl-D-glucosamine biosynth.
PC2 (9.38%)
PC1 (26.01%)
C
Pathway Enrichment
No UTI History
rUTI Remission
D-galactose deg. V
glucose & xylose deg.
L-rhamnose deg. I
heterolactic ferm.
L-1,2 propanediol deg.
glucose & glucose 1-P deg.
glycerol deg.
fucose deg.
β D-glucuronide & D-glucuronate deg.
2-methylcitrate cycle II
cinnamate & hydroxycinnamate deg.
2-methylcitrate cycle I
3-phenyl/hydroxyphenylpropeonate deg.
sulfoglycolysis
3-phenylpropanoate to 2-oxopent-4-enoate
Carbohydrate
ubiquinol 8 biosynth.
ubiquinol 7 biosynth.
ubiquinol 10 biosynth.
ubiquinol 9 biosynth.
menaquinol 6 biosynth. I
menaquinol 9 biosynth.
menaquinol 10 biosynth.
demethylmenaquinol 9 biosynth.
Electron Trans.
L-lysine biosynth. II
L-theronine biosynth.
L-ornithine biosynth.
L-arginine deg. II
L-tryptophan deg.
A.A.
LPS biosynth.
colanic acid biosynth.
ADP L-glycero β D-manno heptose biosynth.
GDP mannose derived O-antagen biosynth.
Cell Envelope
coenzyme A biosynth. I
panothenate & coenzyme A biosynth. I
thiamine diphosphate biosynth. I
thiamine diphosphate biosynth. II
Vitamin
4-deoxy L-threo hex-4-enopyranuronate deg.
hexuronide & hexuronate deg.
D-fructuronate deg.
P.S.
ppGpp biosynth.
Misc.
LDA Score
D
Pathway Enrichment
No UTI History
rUTI Relapse
UDP N-acetyl D-glucosamine biosynth. I
pyruvate ferm. to acetate & lactate II
L-rhamnose deg. I
glycolysis III from glucose
fucose deg.
glyoxylate cycle
hexitol ferm.
TCA cycle IV
TCA cycle V
glycolysis I from G6P
glucose & G1P deg.
fucose and rhamnose deg.
Carbohydratre
adenosine nucleotide biosynth. I
adenosine nucleotide biosynth. II
guanosine nucleotide biosynth. II
pyrimidine deoxyribonucleotide biosynth. III
pyrimidine deoxyribonucleotide biosynth. I
adenosine deoxyribonucleotide biosynth. II
guanosine deoxyribonucleotide biosynth. II
guanosine nucleotide deg. III
adenosine nucleotide deg. II
Nucleotide
L-lysine biosynth. II
threonine biosynth.
L-isoleucine biosynth I.
L-phenylalanine biosynth.
L-aspartate & L-asparagine biosynth.
L-tyrosine biosynth.
A.A.
peptidoglycan maturation
anhydromuropeptides recycling
dTDP-N-acetylthomosamine biosynth.
CMP-3-deoxy D-manno octulosonate biosynth. I
phospholipid biosynth. I
Cell Envelope
D-fructuronate deg.
4-deoxy L-threo hex-4-enopyranuronate deg.
P.S.
S-adenosyl L-methionine cycle I
methylerythritol phosphate pathway I
NAD salvage pathway II
enterobactin biosynth.
sulfate reduction I assimilatory
cis vaccenate biosynth.
Misc.
LDA Score

Figure 7

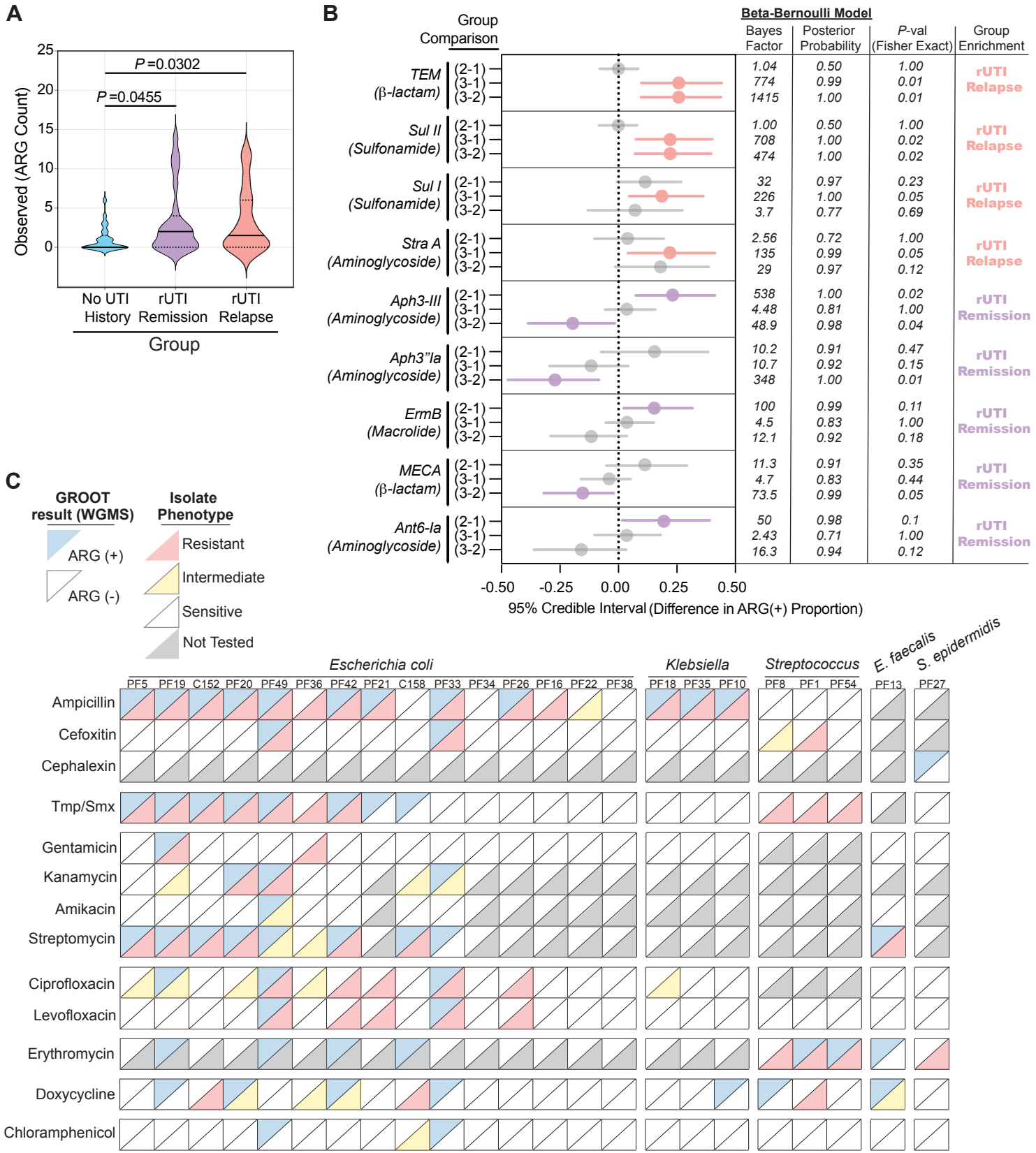
A
Observed (ARG Count)
P =0.0302
P =0.0455
No UTI History
rUTI Remission
rUTI Relapse
Group
B
Group Comparison
Beta-Bernoulli Model
Bayes Factor
Posterior Probability
P-val (Fisher Exact)
Group Enrichment
TEM (β-lactam)
Sul II (Sulfonamide)
Sul I (Sulfonamide)
Stra A (Aminoglycoside)
Aph3-III (Aminoglycoside)
Aph3"Ia (Aminoglycoside)
ErmB (Macrolide)
MECA (β-lactam)
Ant6-Ia (Aminoglycoside)
(2-1)
(3-1)
(3-2)
1.04 0.50 1.00 rUTI Relapse
774 0.99 0.01
1415 1.00 0.01
1.00 0.50 1.00 rUTI Relapse
708 1.00 0.02
474 1.00 0.02
32 0.97 0.23 rUTI Relapse
226 1.00 0.05
3.7 0.77 0.69
2.56 0.72 1.00 rUTI Relapse
135 0.99 0.05
29 0.97 0.12
538 1.00 0.02 rUTI Remission
4.48 0.81 1.00
48.9 0.98 0.04
10.2 0.91 0.47 rUTI Remission
10.7 0.92 0.15
348 1.00 0.01
100 0.99 0.11 rUTI Remission
4.5 0.83 1.00
12.1 0.92 0.18
11.3 0.91 0.35 rUTI Remission
4.7 0.83 0.44
73.5 0.99 0.05
50 0.98 0.1 rUTI Remission
2.43 0.71 1.00
16.3 0.94 0.12
-0.50 -0.25 0.00 0.25 0.50
95% Credible Interval (Difference in ARG(+) Proportion)
C
GROOT result (WGMS)
ARG (+)
ARG (-)
Isolate Phenotype
Resistant
Intermediate
Sensitive
Not Tested
Escherichia coli
PF5 PF19 C152 PF20 PF49 PF36 PF42 PF21 C158 PF33 PF34 PF26 PF16 PF22 PF38
Klebsiella
PF18 PF35 PF10
Streptococcus
PF8 PF1 PF54
E. faecalis
PF13
S. epidermidis
PF27
Ampicillin
Cefoxitin
Cephalexin
Tmp/Smx
Gentamicin
Kanamycin
Amikacin
Streptomycin
Ciprofloxacin
Levofloxacin
Erythromycin
Doxycycline
Chloramphenicol